BNL 50472

HYDROGEN STORAGE AND PRODUCTION IN UTILITY SYSTEMS

SECOND ANNUAL PROGRESS REPORT

F.J. SALZANO, Editor

August 1975

ENGINEERING AND SYSTEMS DIVISION
DEPARTMENT OF APPLIED SCIENCE

BROOKHAVEN NATIONAL LABORATORY
ASSOCIATED UNIVERSITIES, INC.

UNDER CONTRACT NO. E(30-1)-16 WITH THE
UNITED STATES ENERGY RESEARCH AND DEVELOPMENT ADMINISTRATION

DISCLAIMER

BNL 50472
(General, Miscellaneous, and
Progress Reports - TID-4500)

HYDROGEN STORAGE AND PRODUCTION IN UTILITY SYSTEMS

SECOND ANNUAL PROGRESS REPORT
JULY 1, 1974, TO JUNE 30, 1975

F.J. SALZANO, Editor

August 1975

Contributors

C. Braun	J. Milau
E. Cherniavsky	M. Miles
A. Fischer	J. Reilly
K. Hoffman	G. Singh
R. Isler	S. Srinivasan
J. Johnson	G. Strickland
G. Kissel	C. Waide
P. Lu	R. Wiswall, Jr.
S. Majeski	W. Yu

RESEARCH CARRIED OUT AT BROOKHAVEN NATIONAL LABORATORY
UNDER CONTRACT WITH THE UNITED STATES ENERGY RESEARCH
AND DEVELOPMENT ADMINISTRATION
AND WITH
PARTIAL SUPPORT FROM THE EMPIRE STATE ELECTRIC ENERGY
RESEARCH CORPORATION

BROOKHAVEN NATIONAL LABORATORY
UPTON, NEW YORK 11973

Printed in the United States of America
Available from
National Technical Information Service
U.S. Department of Commerce
5285 Port Royal Road
Springfield, VA 22161
Price: Domestic $6.50; Foreign $9.00;
Microfiche $2.25

August 1975 400 copies

HYDROGEN STORAGE AND PRODUCTION IN UTILITY SYSTEMS

Second Annual Progress Report

July 1, 1974 to June 30, 1975

TABLE OF CONTENTS

*Not Scheduled

TABLE OF CONTENTS (Continued)

TABLE OF CONTENTS (Continued)

Figures

TABLE OF CONTENTS (Continued) Page

TABLE OF CONTENTS (Continued) Page

TABLE OF CONTENTS (Continued) Page

TABLE OF CONTENTS (Continued) Page

FOREWORD

This is the second annual progress report describing a program supported by the U.S. Energy Research and Development Administration, Division of Conservation Research and Technology, (ERDA-CRT) Chemical Storage Branch, for the development of the technology of electrolytic hydrogen production, storage, and reconversion to electricity. The program was initiated on November 1, 1973. The emphasis is on the improvement in the cost and efficiency of electrolytic hydrogen production and the use of metal hydrides for hydrogen storage. The scientific basis for the use of metal hydrides for hydrogen storage was established in a program at the Brookhaven National Laboratory under way since 1967 and now supported by the Energy Research and Development Administration, Division of Molecular Science. The primary goal of this program is the development of the technology, hardware, and technical skills required to apply the technique of using metal hydrides, namely iron titanium, to the problem of electric energy storage, and in the general application of hydrogen in selected sectors of the U.S. energy system. Design work on a full-scale storage plant has been initiated along with systems analysis studies of energy storage in utility systems. Engineering tests, hardware design, and laboratory studies in support of the engineering development program are in progress.

Prior to the initiation of the ERDA-DES program, construction was begun on a metal hydride storage reservoir for the Public Service Electric and Gas Company of New Jersey (PSE&G). A system which holds approximately 14 lb of hydrogen was delivered and installed at PSE&G, and is currently being operated by the utility as part of an electric energy storage experiment.

This program is now supported jointly by the ERDA-CRT and the Empire State Electrical Energy Research Corporation (ESEERCO), a group of the major New York State utilities that sponsor research related to the needs of electric utilities. ESEERCO is supporting work on a specific test bed project which is described in Task Group 3.1 - Engineering Test Beds.

In order to facilitate the speedy preparation of the quarterly and annual reports, the report is divided into distinct sections corresponding to the major areas of work in the program. Identification of figures and tables related to each area is facilitated by a prefix added to the figure or table number. For example, Table 2-3 corresponds to work in Area 2 - Hydrogen Production and Auxiliaries.

INTRODUCTION

The Hydrogen Energy Storage Program is concerned with the development of an integrated hydrogen production, storage, and reconversion system designed for peak electric service by electric utilities. This concept appears to be a very promising and flexible alternative to pumped storage and peaking gas turbines which are limited by lack of suitable sites and the inefficient use of high-grade fossil fuels, respectively. When a hydrogen production and storage system is coupled with a conversion device, such as a fuel cell or gas turbine, it is possible to operate the conversion device in both a storage and generating mode. Thus, a hydrogen electric storage system can be operated as a "Dual Mode" device using off-peak electric capacity in the storage mode or in the generating mode using distillate fuel. Operation in the "Dual Mode" allows better seasonal matching with available off-peak capacity and offers a greater degree of flexibility to a utility than a passive storage device. It also allows the possible use of hydrogen produced from off-peak power as a supplement to the natural gas supply. Quantities of hydrogen up to 10% can be injected into existing natural gas systems allowing the flow of nuclear or solar energy into the U.S. natural gas supply.

The Energy Research and Development Administration, Division of Conservation Research and Technology, Chemical Storage Branch (ERDA-CRT-CSB) is supporting this program which has the goal of developing the technology, hardware, and technical expertise necessary for improving the efficiency reducing the cost of electrolytic hydrogen production and secondly, to apply the technique of using metal hydrides, namely iron titanium, for hydrogen storage. Although in the storage work the emphasis is on the application of metal hydrides, other hydrogen storage options, high-pressure gas and liquid hydrogen are given due consideration. The program recognizes that the development of a low-cost efficient method of hydrogen production is essential if nuclear and solar energy sources are to be used to supply some of the fuel needs of the future, presently supplied by natural gas and petroleum.

A preliminary Management Program was prepared at the initiation of the program to assist in coordinating the diverse design and development activities required to achieve the

program goals in an orderly and efficient manner. This plan has been updated to reflect progress and new task initiatives.

The program has been organized into five major areas. The first deals with the Engineering Analysis and Design Activity which provides an integrative function. The next three areas cover the development activity on production, storage, and conversion, respectively, while the last area comprises the Prototype and Demonstration Facilities that are planned. With respect to each of the development areas, the research approach varies considerably. The Production Area involves both Brookhaven and contractor development work, as does the Storage Area. In the Conversion Area, on the other hand, the major activity is going on in industry quite independent of the Brookhaven program. Our efforts are directed primarily towards maintaining close contact with that work, encouraging developmental efforts which relate to this program, and studying the integration of conversion components into the overall system. A list of the five areas follows:

Area 1. Engineering Analysis and Design
Area 2. Hydrogen Production and Auxiliaries
Area 3. Hydrogen Storage Development
Area 4. Electric Generating Systems and Auxiliaries (Fuel Cell, Turbines, etc.)
Area 5. Facilities

A detailed description of the scope of activities in each of the major areas is given in Appendix A which is included as a part of each progress report. Each major area in the Management Plan is broken down according to the associated task groups and identified with a numerical notation where the unit place represents the major area and the decimal place identifies a particular task group. For example, 1.1 corresponds to Area 1, Engineering Analysis and Design and Task Group 1.1 is the first task and deals with Program Planning and Management. A complete list of the major areas and associated task groups is given in the schedule in Appendix B. The format of all progress reports is to state progress in each of the major areas according to the numbered task groups. The scope of the activity associated with each task

group will be stated in each report along with progress reported in connection with that task group. A list of the major milestones for the program through Fiscal Year 1976 is given in Appendix C.

The revised Management Plan (HES-2) should be consulted regarding further breakdown of the task groups into more detailed subtasks involving specific activities of shorter duration being performed by individuals or groups charged with a specific responsibility such as: design, fabrication, calibration, operation, etc.

The problem of technology transfer is recognized and the tasks have been structured so as to involve the eventual user, designers, and material suppliers throughout the course of the program. A start was made in connection with this need when a cooperative program with the Public Service Electric and Gas Company of New Jersey to build an iron titanium hydrogen storage tank holding a minimum of ten pounds of hydrogen was initiated early in 1973. Also, a portion of the present funding comes from the Empire State Electrical Energy Research Corporation (ESEERCO). Efforts to encourage technology transfer in the use of metal hydrides for hydrogen storage is a continuing effort during the course of the program. Appendix D is a list of the current subcontracts in progress which relate to the prime objectives of the program.

PUBLICATIONS

M. Lotker, E. Fein, and F. J. Salzano, The Hydrogen Economy--A Utility Perspective, Pres. at the IEEE PES Winter Meeting, New York, New York, January 27-February 1, 1974, #C74099-8 (BNL 19267).

J. A. Casazza, R. A. Huse, V. T. Sulzberger, and F. J. Salzano, Possibilities for Integration of Electric, Gas, and Hydrogen Energy System, Proc. of the Conference Internationale de Grands Reseaux Electriques a Haute Tension, Paris, France, August 21-29, 1974 (BNL 19268).

G. Strickland, J. J. Reilly, and R. H. Wiswall, An Engineering Scale Energy Storage Reservoir of Iron Titanium Hydride, Pres. at the Hydrogen Economy Miami Energy (THEME) Conference, Coral Gables, Florida, March 18-20, 1974 (BNL 18634).

F. J. Salzano, R. J. Isler, E. A. Cherniavsky, and K. C. Hoffman, On the Role of Hydrogen in Electric Energy Storage, ibid (BNL 18721).

W. S. Yu, E. Suuberg, and C. H. Waide, Modeling Studies of Fixed Bed Metal Hydride Storage Systems, ibid (BNL 18720).

J. R. Powell, F. J. Salzano, and W. A. Sevian, The Technology and Economics of Hydrogen Production from Fusion Reactors, ibid (BNL 18718).

C. H. Waide, J. J. Reilly, R. H. Wiswall, and K. C. Hoffman, The Application of Metal Hydrides to Ground Transport, ibid (BNL 18719).

J. Reilly, K. Hoffman, G. Strickland, R. Wiswall, Iron Titanium Hydride as a Source of Hydrogen Fuel for Stationary and Automotive Applications, Pres. at the 26th Power Sources Symposium, Atlantic City, New Jersey, April 29-May 2, 1974 (BNL 18651).

J. J. Reilly and R. H. Wiswall, Jr., Formation and Properties of Iron Titanium Hydride, Inorganic Chem. 13, 1 (1974).

G. Strickland and J. J. Reilly, Operating Manual for the PSE&G Hydrogen Reservoir Containing Iron Titanium Hydride, February 1974 (BNL 18725).

J. M. Burger, P. A. Lewis, R. J. Isler, F. J. Salzano, and J. M. King, Jr., Energy Storage for Utilities via Hydrogen Systems, Pres. at the 9th Intersociety Energy Conversion Engineering Conference, San Francisco, California, August 26-30, 1974 (BNL 19266).

J. J. Reilly, R. H. Wiswall, K. C. Hoffman, and C. H. Waide, Metal Hydrides as Hydrogen Storage Media, Pres. at the 7th Alternative Automotive Power Systems Division Contractors Coordination Meeting, Ann Arbor, Michigan, May 1974 (BNL 18887).

R. J. Isler, F. J. Salzano, E. M. Suuberg, and W. S. Yu, Reference Design of a 26 MW(e) Electric Energy Storage System, A Preliminary Report, July 1974 (BNL 19231).

F. J. Salzano and E. A. Cherniavsky, Program Goals and Justification for Energy Storage Program, A Preliminary Technology Assessment prepared for the Division of Applied Technology, U.S. AEC, August 1, 1974.

W. A. Sevian and F. J. Salzano, Systems Study of Two Synthetic Transportation Fuel Options, Proc. of the American Electrochemical Society Meeting, New York City, October 13-17, 1974, pp. 594-8 (BNL 20071).

J. R. Powell, F. J. Salzano, W. S. Yu, and J. S. Milau, The Application of High Efficiency Power Conversion Cycles to Nuclear Reactors, Pres. at the 1975 American Nuclear Society Meeting, New Orleans, Louisiana, June 8-13, 1975 (BNL 19698).

M. H. Miles, Evaluation of Electrocatalysts for Water Electrolysis in Alkaline Solutions, J. Electroanalytical Chemical and Interfacial Electrochemistry 53 (1975). (In press)

M. H. Miles, G. Kissel, P. W. T. Lu, and S. Srinivasan, Effect of Temperature on Electrode Kinetic Parameters for Hydrogen and Oxygen Evolution Reactors in Alkaline Solutions, Pres. at the 147th Meeting of the Electrochemical Society, Toronto, Canada, May 1975 (BNL 19684).

C. Braun, E. A. Cherniavsky, and F. J. Salzano, The Economic Incentive for Introducing Electric Storage Devices into the National Energy System, Pres. at the 10th Intersociety Energy Conversion Engineering Conference, Newark, Delaware, August 17-22, 1975, (BNL 20231).

J. R. Powell, F. J. Salzano, W. S. Yu, and J. S. Milau, High Efficiency Power Conversion Cycles Using Hydrogen Compressed by Absorption on Metal Hydrides, Pres. at the 10th Intersociety Energy Conversion Engineering Conference, Newark, Delaware, August 17-22, 1975 (BNL 19645).

G. Kissel, P. W. T. Lu, M. H. Miles, and S. Srinivasan, Hydrogen Production by Water Electrolysis--Methods for Approaching Ideal Efficiencies, Pres. at the 10th Intersociety Energy Conversion Engineering Conference, Newark, Delaware, August 17-22, 1975 (BNL 19677).

J. R. Powell, F. J. Salzano, Wen-Shi Yu, and J. S. Milau, High Efficiency Power Cycles Using Metal Hydride Compressors, January 1975, (BNL 50447).

C. Braun, E. A. Cherniavsky, and F. J. Salzano, Energy Storage Systems Analysis for the U.S. Energy Research and Development Administration, Topical Report, Allowed Costs for the Introduction of Electric Storage Devices into the National Energy System, April 1975.

S. Srinivasan, Electrocatalysts for Water Electrolysis and Fuel Cells, Presented at the Fuel Cell Catalysis Workshop, Electric Power Research Institute, Palo Alto, California, January 15-17, 1975.

S. Srinivasan, Energy Storage for Electric Utilities Using Hydrogen, Presented at Middle Tennessee State University, Murfreesboro, Tennessee (Chem. Seminar), February 18, 1975.

THIS PAGE

WAS INTENTIONALLY

LEFT BLANK

useful reference electrode system is available. A transient method for obtaining Tafel plots has been developed which facilitates the rapid measurement of electrocatalytic activities of prospective electrode materials. These techniques and others are being used to study the catalytic behavior of various nickel based alloys for use in alkaline water electrolysis systems. Similar work on noble metal alloys systems for use in acid (solid polymer) electrolyte system is being carried out at BNL and via subcontract to the Middle Tennessee State University.

A number of prospective barrier materials for use in alkaline electrolysis systems have been screened in equipment built during FY 1975. Potassium titanate has been identified as a promising candidate separator material which would allow operating temperatures of 150°C in alkaline systems.

A BNL subcontract has been given to the General Electric Company for the design of a hydrogen production plant based on the solid polymer electrolyte concept and which would be suitable for use in a 26MW(e) hydrogen electric storage plant, i.e., the Reference Design hydrogen electric storage plant being developed under subcontract to Burns & Roe.

Area 3 - Hydorgen Storage Development

Test Bed A-1, for long term attrition studies, was operated for 1200 hydride-dehydride cycles. About 60% of the starting FeTi alloy, VE 524, suffered a factor of ten size reduction whereas the ability to absorb hydrogen showed no decrease. This bed was also used to obtain both kinetic and equilibrium data on the same batch of commercial FeTi material after repeated cycling.

Test Beds A-1-1 and A-1-2 were constructed and put into operation to further study attrition. Bed A-1-1 has 16 mesh starting material and has completed about 1360 cycles. Bed A-1-2 uses 100 mesh starting material and has completed 1460 cycles. NO-1 FeTi alloy from National Lead is the starting material for both beds.

An aluminum vessel was constructed to decrease the Δt in the vessel (improve heat transfer) and to gain experience with aluminum as a potential container material. This bed has been used to study the hydriding pressure versus composition curve of NL-1

material and will also be used for impurity additive studies and hydriding/dehydriding dynamic studies.

The 10-lb hydrogen reservoir (FeTi) built for Public Service Electric and Gas Company of New Jersey has continued to function without difficulty in their hydrogen-energy storage test facility, and we have maintained liaison with them, mainly by reviewing data supplied to us. Operation of the reservoir, which is coupled to an electrolyzer and a fuel cell, is now routine and ten complete charge and discharge runs were successfully completed. The reservoir was operated at hydrogen transfer rates of 1.4 - 1.5 lbs/hr and is capable of delivering 13 pounds of hydrogen at the above rate.

The design and construction was completed on the 6-in.-diameter test bed which contains 84 pounds of iron titanium alloy and is capable of storing 1.2 pounds of hydrogen as a hydride. This device represents a simple heat transfer cell, as would exist in the Reference Design B concept, from which thermal and kinetic data will be obtained for use in the design of larger fixed bed internal heat exchange type reservoirs. The vessel is 2.5 feet long, has an axial porous metal tube for the particle barrier, is provided with 21 internal thermocouples, and an external jacket through which cold or hot water is circulated to handle the thermal load during the charging or discharging of hydrogen. Following activation of the alloy to produce the initial hydride, the first discharge run was successfully made. This reservoir is known as the ESEERCO Test Bed because of support contributed by the Empire State Electric Energy Research Corporation for the construction and operation of this engineering test bed.

Although the 300-series stainless steels are now used successfully for the construction of small-scale hydride storage equipment, they are too costly for use in large-scale plants and must be replaced by low cost steels which are resistant to hydrogen embrittlement and excessive loss of ductility. A cooperative program to identify suitable materials was initiated with Sandia Laboratories. Screening tests of candidate metals in pressurized hydrogen were begun at Sandia, and the design and construction of equipment for exposing test specimens in the iron titanium hydride environment were started at Brookhaven. Eighty self-loaded tensile

specimens of two common steels, an alloy steel, an aluminum alloy and a stainless steel will be exposed. These plain, notched and welded forms will be evaluated at their proof stress level, i.e., the highest stress expected in ordinary operations.

Evaluation of potential safety hazards presented by FeTi as a hydrogen storage media has been evaluated by means of in-house work and subcontract to the Denver Research Institute. No unexpected hazards have been identified.

Work to develop a commercial vendor for iron titanium has progressed and a subcontract has been given to the International Nickel Company to assist in the development of a specification for large quantities of material which could be produced in a commercial process. Commercial prepared material received from "Timet" a subsidiary of NL Industries has been shown to approach the behavior of zone refined FeTi. Optimization work on Reference Design B has identified the desired characteristics of FeTi, i.e., pressure, temperature composition and hysteric behavior. Laboratory studies have identified a ternary composition containing manganese which is close to meeting the optimal design requirements and exhibits appreciably reduced hysteresis.

Area 5 - Facilities

It has been decided that the Prototype Test Facility (PTF) will utilize the Reference Design B scheme, i.e., fixed bed with internal heat exchange. The hydrogen storage reservoir for the PTF will have a 50kW thermal equivalent power rating and a 500kW hour thermal equivalent hydrogen capacity. A process instrumentation diagram has been prepared and design work is in progress.

PAST PROGRESS REPORTS

F. J. Salzano, Editor, Hydrogen Storage and Production in Utility Systems, First Quarterly Progress Report, November 1 to December 31, 1973, BNL 18603, January 1974.

F. J. Salzano, Editor, Hydrogen Storage and Production in Utility Systems, Second Quarterly Progress Report, January 1 to March 31, 1974, BNL 18920, April 1974.

F. J. Salzano, Editor, Hydrogen Storage and Production in Utility Systems, First Annual Report, November 1, 1973 to June 30, 1974, BNL 19249, July 1974.

F. J. Salzano, Editor, Hydrogen Storage and Production in Utility Systems, Third Quarterly Progress Report, July 1 to September 30, 1974, BNL 19520, October 1974.

F. J. Salzano, Editor, Hydrogen Storage and Production in Utility Systems, Fourth Quarterly Progress Report, October 1 to December 31, 1974, BNL 20040, January 1975.

F. J. Salzano, Editor, Hydrogen Storage and Production in Utility Systems, Fifth Quarterly Progress Report, January 1 to March 31, 1975, BNL 20420, April 1975.

PROGRESS IN AREA 1: ENGINEERING ANALYSIS AND DESIGN

Task Group 1.1 Program Planning and Management

Scope: This Task Group includes all the tasks required to prepare and update a management plan in sufficient detail to assist in the attainment of the project goals in an efficient and economical manner. Manpower requirements, costs estimates, and schedules are included in the plan. The program plan defines the separate tasks or groups of tasks in the overall program and indicates their impact on the program.

The monitoring of the technology transfer effort in the program is an extremely critical activity in this Task Group. Provisions have been made in each program area to obtain the necessary utility, architect engineer, and contractor involvement that is required to ensure that the ultimate system will be implemented as easily as possible. Safety and reliability are also recognized as being important to public acceptance. Again these factors will be addressed in each program area and will be monitored as part of the work in this Task Group.

The preparation of progress reports and budget material is also included in this Task Group.

Progress During the Report Period: The Management Plan (HES-2) has been revised to reflect progress during the past year and one new task initiated, i.e., Task 3.4--The Selection of Container Materials--has been added. The need for this activity was demonstrated via discussions with Sandia regarding the available information required to select container materials for a metal hydride storage facility. Sandia is a participant in this effort.

The projected program schedule has been revised and is shown in Appendix B. These changes and the revised set of projected milestones in Appendix C reflect new initiatives and minor changes in priorities and direction indicated during the fiscal year.

Liaison with the interested electric utilities has continued. Contact and discussion have been underway with prospective fuel cell supplies; however, funds were not available in FY 1975 to initiate any subcontract efforts regarding conversion devices for electric storage systems.

In anticipation of the program schedule, a major effort was made to make contact and initiate discussions with prospective suppliers of water electrolysis equipment. Electrolyzer equipment options for the Prototype Test Facility (PTF) will be examined in the new fiscal year.

A new initiative on the development of ternary iron titanium alloys with more desirable properties than the pure iron titanium alloys for storage applications has been programmed into the present effort. This is in accord with the program goal of achieving the lowest cost storage technology.

A number of subcontracts relevant to the program objective have been placed and the general scope of these efforts and the participating contractors are listed in Appendix D.

The schedule for the PTF has been pushed forward to more closely follow the schedule of work in Task 3.4 on the selection of container materials.

Based on energy storage system studies and recent design efforts, it appears desirable to maximize the utilization of the fuel cell or other conversion devices and hydrogen production equipment. As such, we have begun to examine more closely the "dual mode" concept where the fuel cell or other conversion device can be a generating device using distillate fuel or operate in an electric storage mode using hydrogen produced from off-peak power. This allows for better use of high cost capital facilities than a straight electric-to-electric storage system, it offers great operating flexibility, good seasonal matching with availability of off-peak power and the option of injecting some of the hydrogen produced into a utilities natural gas supply as required. In this scheme, the fuel cell can serve both as an intermediate load and peaking device operating for storage or direct generation, via hydrogen or distillate fuels respectively. This makes for

effective utilization of the fuel cell. Also, the stored hydrogen can be used to improve the load carrying ability of the fuel cell distillate oil reformers by by-passing stored hydrogen around a base loaded reformer to meet a varying load.

Task Group 1.2 Reference Designs of Demonstration Facility

Scope: This task contains the activities necessary to prepare reference designs for the demonstration storage facility. The initial design will be based on estimated performance and as data become available from the development work, the design will be revised. The use of liquid hydrogen and pressurized hydrogen gas as storage schemes will be examined with respect to the reference design.

Progress During the Report Period: The design of the electric energy storage system proposed in an earlier report (BNL-19231, July 1974) has been developed in conjunction with Burns and Roe, Inc. In this design, designated Reference Design "A", the temperature of the iron titanium beds is controlled by circulating gaseous hydrogen with the heat transfer done in external gas to water heat exchangers in series with the beds.

The development of Reference Design "A" at this time identifies the areas holding the most promise for future research and development, and provides a state-of-the-art design with which to compare competing technologies.

Figure 1-1 is a flow schematic for the overall plant process. During the hydriding phase, high voltage, 3-phase, ac power from the utility power network is transformed and rectified by solid state rectifiers, to dc power. The dc power is supplied to water electrolyzers to produce hydrogen and oxygen. The oxygen is released to the atmosphere, while the hydrogen is cooled and passed through a deoxygenator to remove residual oxygen. The hydrogen is then passed through a dryer to remove residual water vapor and produce hydrogen gas with a dew point of $-76^{\circ}F$ (referred to atmospheric pressure). The dry gas is fed to the circulating hydrogen loop to be cooled and absorbed in the hydride beds.

Figure 1-2 shows the pressure-temperature conditions, the operating flow rates, and other characteristics in the circulating hydrogen loop at the initiation of hydriding. As the hydride cools, the bed exit temperature decreases. At the same time, the temperature difference in the cooler decreases correspondingly, since the bed entrance temperature remains constant for all practical purposes. As a consequence, to maintain a constant cooling duty (and hydriding rate), the hydrogen circulation rate must increase. Additional pumping capacity, which increases the rate by a factor of about 2, is included.

Figure 1-3 shows the pressure-temperature conditions in the circulating hydrogen loop at the termination of dehydriding. Similar to the hydriding process, during dehydriding the circulation rate must be varied to maintain a uniform hydrogen liberation rate, since the hydride bed exit temperature increases from 113°F to 160°F. Additional pumping capacity, with a turn-up rate of about 2, is therefore included.

At the initiation of the dehydriding process, the shutoff valve in the line from the electrolyzers is closed and the valve in the line to the fuel cell packages is opened. The temperature and pressure of the hydrogen leaving the hydride beds must be adjusted, since the fuel cell packages require an inlet temperature of about 300°F and pressure not much higher than 1 atmosphere. Consequently, the hydrogen is heated to 300°F, using rejected heat from the fuel cell packages, throttled to a pressure slightly higher than 1 atmosphere, and then piped to the fuel cells. In the fuel cells, hydrogen and air are electrochemically combined to produce 25,000 lbm H_2O/hr and 27.6 MW(e) of dc power. The dc power is fed to a solid state inverter-transformer which converts it to 3-phase ac power at the voltage level required by the load or existing power network. The Reference Design "A" plant cycle is 10 hours of hydriding and 10 hours of dehydriding during a 24-hour period.

Figure 1-4 shows the estimated nominal plant performance. During the hydriding portion of the plant cycle, the gross electrical power input is 72.5 MW(e) 3-Ø, ac. Auxiliaries such as the hydrogen circulators, cooling tower pumps, etc., require an estimated 0.7 MW(e) leaving 71.8 MW(e) 3-Ø ac to power the

solid state rectifiers. The rectifiers have an estimated conversion efficiency of about 97 percent, so 2.16 MW are rejected to the atmosphere as heat and about 70.0 MW(e) dc are distributed to the 24 electrolyzers. The electrolyzers convert the 70.0 MW(e) into 2800 lbm-H_2/hr with a conversion efficiency of about 72 percent, based on the higher heating value of hydrogen (611000 Btu/lbm). About 20.0 MW of heat are rejected directly and through the circulating cooling water system to the atmosphere. The 2800 lbm/H_2/hr produced by the electrolyzers are charged into the hydride beds at a uniform rate with an assumed efficiency of 100 percent. The heat of hydriding is rejected to the atmosphere by means of the circulating hydrogen and cooling water systems. The chemical energy of the hydrogen is thus stored at the rate of 50.1 MW, based on the higher heating value of hydrogen, and the nominal hydriding effectiveness for the charging portion of the plant cycle, defined as the ratio of the rate of hydrogen chemical energy stored to the total plant power required and is 69 percent.

During the discharging cycle or dehydriding, hydrogen is liberated from the hydride beds at a uniform rate of 2800 lbm-H_2/hr. The heat of hydriding, 5.54 MW(t), is supplied, for normal operation by the heat rejected by the fuel cells, which are assumed to operate with a conversion efficiency of 55 percent, based on the higher heating value of hydrogen. In addition, about 0.44 MW of heat from the fuel cell packages are also used to preheat the hydrogen before it enters the fuel cells to prevent quenching the electrochemical reactions. From the 50.1 MW rate of hydrogen chemical energy input to the fuel cells (2800 lbm-H_2/hr), therefore, 27.6 MW(e) dc is extracted and 22.6 MW(t) is rejected. As noted, 5.54 MW and 0.44 MW of the rejected power are utilized, while the remainder is transferred directly to the atmosphere. The 27.6 MW(e) dc is distributed to the SCR inverters, which have an estimated conversion efficiency of 97 percent, and converted to 26.7 MW(e) ac with about 0.90 MW of heat rejected to the atmosphere. About 0.7 MW(e) of the 26.7 MW(e) is used to power auxiliaries during dehydriding leaving a net plant output of 26.0 MW(e) 3-Ø, ac. Thus, the nominal dehydriding effectiveness for the power generation portion of the plant cycle, defined as the ratio of the net plant output to the rate of hydrogen chemical energy available, is 52 percent. For the

complete plant operating cycle, therefore, the efficiency, or ratio of net plant output to total plant input, is 36 percent.

The site plan shown in Figure 1-5 includes many items not normally considered in the early stages of process development but necessary to establish a true distribution of costs and areas for the base case.

The plan indicates that about 16 acres of land are required. The electrolyzers are housed in a separate building to protect them from the weather. The fuel cell packages do not require a building, since each includes a weatherproof covering. The electrolyzer building and fuel cell packages are located close to one another so that shared electrical equipment, such as switch-gear and power transformers, can be grouped. This arrangement also minimizes the length of high current bus required from the low sides of the transformers to the rectifiers and inverters. The administration building houses the instrumentation and control equipment required to control and monitor the plant operations, and to perform periodic tests to verify hydrogen purity, water quality and hydride condition. The makeup water treatment and boiler house is adjacent to the administration building. A 10,000 gallon tank is provided for fuel oil storage to serve the boilers, and a 40,000 gallon condensate tank is provided for storage of makeup water, water drained from the fuel cell packages, and condensate from the steam system, prior to recycling it to the electrolyzers and boilers. A 200,000 gallon waste treatment pond is provided nearby to hold chemical wastes and to permit treatment prior to disposal. A fire protection water tank and fire pumps are located near the plant boundary. Fire hydrants are provided throughout the plant to cover all areas. A mechanical draft cooling tower is included to provide cooling water for the cooling requirements of the electrolyzers, hydride beds, and other plant equipment.

Further details of the arrangement are shown in Figures 1-6 and 1-7. Provisions are included for truck delivery of caustic potash (KOH) electrolyte to the site, and transfer to a 10,000 gallon storage tank located adjacent to the electrolyzer building. A 200,000 gallon electrolyte drain and dump tank is provided adjacent to the electrolyzer building.

The tank is sized to hold the electrolyte from the entire electrolyzer system when it is necessary to shut the plant down. A 100-ton bridge crane is provided in the electrolyzer building for maintenance and handling of the electrolyzers. Two truck bays and work areas are also provided, one at each end of the building. Each of the electrolyzers receives dc electrical power from a separate rectifier. The 24 rectifiers are located in a temperature controlled rectifier room from which high current electrical bases run.

In the hydrogen storage area, the 10 hydride beds are located outdoors on concrete foundations. Three concrete pedestals are provided for each tank. The hydrogen circulators, deoxygenator and dryer are located in a small building adjacent to the tanks to protect them from the weather and preclude potential freezing problems.

The fuel cell packages are mounted on a concrete foundation in the fuel cell area. A three-foot separation is provided on both sides of each package for clearance. All pipe and electrical connections are made to one face of each fuel cell package, so that clear access is available at the opposite one for installation or removal. A service apron is provided for trucks and a mobile crane which could be brought on site for service operations. The electrical output from each group of six fuel cell packages is fed, via a high current bus, to a corresponding group of six inverters located near the fuel cell packages. The ac output from the inverters is then fed to four switch-gear packages and the four plant power transformers.

The compartmentalization of the arrangement allows other technologies to be substituted as desired. Minimization of land area to better fit urban economics is premature at this stage of process development.

The distribution of costs for the Reference Design "A" by Federal Power Commission (FPC) accounts is shown in Table 1-1. By far the largest of these accounts is that for processing and storage equipment, representing 72% of the total. The distribution of costs within this account is summarized in Table 1-2. The largest cost segment, 43.3 percent, is

attributed to the electrolyzers. Although the electrolyzers envisioned for this design study represent a developed technology, reductions in capital cost of up to 50% could result from current research and development activities. Fuel cell costs, 14.3 percent, and iron titanium costs, 15.3 percent, while significant would yield proportionally less to capital cost reductions. On the other hand, an increase in fuel cell efficiency would reduce the entire plant size upstream of the cells resulting in even greater cost reduction.

Task Group 1.3 Liaison with Utilities and Major Component Vendors

Scope: This task group includes the tasks required to ensure that the end product of the program is responsive to the needs of the electric utility industry. The status of existing technology and development work for major system components such as fuel cells, turbines, hydrogen compressors, etc. will be obtained. This information will provide a basis for the more detailed investigation of these items covered in program Areas 2 and 4.

Progress During the Report Period: Subcontract work has been initiated by the General Electric Company (GE) on the design of an advanced water electrolysis production plant for the 26 MW(e) energy storage reference design plant. The exact scope of work to be undertaken by GE was given in Appendix F of the Third Quarterly Progress Report, July 1 to September 30, 1974, BNL 19520.

Contact was made with a number of prospective European suppliers of water electrolysis plant and a number of plant sites were visited. A summary of F. J. Salzano's European trip report related to this activity is included in Appendix E of the Fifth Quarterly Progress Report, January 1 to March 31, 1975, BNL 20420.

A subcontract was also initiated with the International Nickel Corporation (INCO). The exact scope of this subcontract activity is given in Appendix F of BNL 20420 (see paragraph above).

Task Group 1.4 Modeling of System Storage and Optimization Studies

Scope: This activity involves dynamic system modeling via computer studies. Particular emphasis will be on the dynamics of the storage system in response to changing load conditions in conversion devices and hydrogen production plants. An effort will be made to do cost optimization of the systems in terms of load conditions, cost of off-peak power, and process variables. This activity interfaces with the engineering design work in connection with the Prototype Test Facility (PTF) and the Demonstration Facility (DF).

Progress During the Report Period: Modeling Studies of Fixed-Bed Metal Hydride Storage Systems: Analytical models for the study of the dynamic behavior of two proposed fixed-bed hydrogen storage systems were developed; a convection bed model and a conduction bed model. The direct heat transfer scheme, termed a convection bed, utilizes a recirculating stream of hydrogen to transport heat to and from the bed by direct contact with the hydride. A heat exchanger, external to the bed, serves as the heat source or sink. The indirect heat transfer scheme, termed a conduction bed, incorporates heat transfer surface in the bed and heat is transferred from a hot fluid to and through the hydride by conduction.

The main output from the modeling work is the temperature and composition profiles in the bed and the hydrogen charging and discharging rates of the system. The modeling work also produced design guidelines for a test facility, and provides data for comparisons between analytical and experimental results.

Routine work is continuing which services the needs of Areas 1.2 and 3.1 the engineering design work and the test bed program, respectively.

Task Group 1.5 Systems Analysis of Energy Storage and Integration of Hydrogen into U.S. Energy Economy

Scope: This task group covers systems analysis and economic studies of energy storage in general and the role of hydrogen in the U.S. energy economy, individual areas of the country, and specific utility systems. This includes specific consideration of the role of hydrogen to supply the peak electric demands and the competition with other storage options. Activities in this area will eventually consider the use of hydrogen as a domestic fuel, i.e., a replacement for natural gas, a transportation fuel and interfacing hydrogen supply systems with both novel and conventional energy sources such as fission, fusion, coal, solar, wind, tidal, and geothermal.

Progress During the Report Period: The Break-even Capital Costs of Electric Storage Devices: The economics of introducing electric storage devices into the year 1985 national energy system are considered in this section. The generalized electric storage device is characterized only by its overall electric-to-electric conversion efficiency, by the load factor, and by the device lifetime, which is reflected in the value of the capital recovery factor utilized in the cost computations. The current series of calculations assumes a 0.15 fixed charge rate and an implicit 30-year lifetime.

The break-even capital cost is calculated as a function of the overall electric-to-electric conversion efficiency, for storage devices operating at three peaking load factors: 0.05, 0.10, and 0.20. In order to calculate the matrix of capital costs, it is necessary to specify the structure of the electric peak demand.

The introduction of the electric storage devices into the national energy system is affected by the relative attractiveness of other electric generating plants available to the system, e.g., gas turbines and hydroelectric plants. In order to investigate the effects of varying the cost of the competing generating plants on the economics of the electric storage devices, the price of the distillate fuel oil available to the entire national energy system was varied. Three different distillate fuel oil prices were considered: the nominal price

of $\$1.3/10^6$ Btu and $\$2.6/10^6$ Btu and $\$3.9/10^6$ Btu, which are double and triple the nominal value.

Each storage scenario investigated results in a three-dimensional set of break-even costs calculated as a function of conversion efficiency, peaking load factor and distillate fuel oil price. The calculated capital costs include an equivalent capitalized operating and maintenance (O and M) cost component. The reported values must be corrected for the specific O and M cost of any storage technology under consideration. The results of the computations for the nominal storage scenario are presented in Table 1-3 and in Figures 1-8 and 1-12. A discussion of the effects of the three basic parameters on the economics of the electric storage devices now follows:

It can be seen from Table 1-3 and Figures 1-8, 1-9 and 1-10, that operation at the 0.20 load factor is the most economic mode of storage device utilization within the national energy system. This is inferred from the fact that the highest break-even capital costs are calculated for operation at this load factor. The lowest capital costs are calculated for power generation at the 0.05 load factor, and the allowed capital costs for operation at the 0.10 load factor fall in between. Thus, in terms of economic order of merit it is most advantageous to operate electric storage devices at the 0.20, 0.10, and 0.05 peaking load factors respectively. This assertion holds at oil prices of $\$2.6/10^6$ Btu and $\$3.9/10^6$ Btu, for storage conversion efficiencies greater than 0.25 to 0.30. At a distillate fuel oil price of $\$1.3/10^6$ Btu the capital cost for operation at 0.20 load factor will be higher than the figures calculated for the 0.10 load factor vs. capital cost trend and is towards high break-even costs as the load factor increases.

As a general rule the break-even capital cost for the electric storage device will increase as the overall electric-to-electric conversion efficiency is improved. This statement is valid at all distillate fuel oil prices and all load factors. The effects of improving the conversion efficiency are more pronounced at high oil prices and at the 0.20 load factor. The most dramatic effect of conversion efficiency improvement on the storage device capital cost occurs in the region of low efficiencies--0.15 to 0.45. More moderate increases in capital cost per unit improvement in conversion efficiency

occur in the region of 0.45 - 0.75. At conversion efficiencies above 0.75 it can be seen that the break-even capital cost for operation at the 0.05 load factor, and also for 0.10 load factor operation, reach a saturation value. The increment in capital cost per unit improvement in conversion efficiency becomes very small. This pattern can be explained by the fact that at the 0.05 and 0.10 load factors the storage device competes primarily against gas turbines which incur high electricity production costs. Storage devices become competitive with direct generating plants even at efficiencies of 0.55. There is no economic incentive to raise the conversion efficiency above 0.75, so far as the power production cost of the competing alternatives remain high.

No saturation effect is evident in the break-even capital cost curve for operation at the 0.20 peaking load factor. Further, there exists an economic incentive, in terms of increased break-even costs, for improving the conversion efficiency even up to values as high as 0.95 - 1.0. This can be attributed to the fact that at the 0.20 load factor the generalized storage device will have to compete against relatively cheap peaking hydro and pumped storage plants. Thus, in order to maintain competitiveness when operating at the 0.20 peaking load factor the storage device efficiency should be increased as much as economically possible.

The effect of increasing the distillate fuel oil price on the break-even capital cost of electric storage plants is shown in Figures 1-11 and 1-12. Generally, as distillate oil prices are increased, the break-even capital cost increases. The most pronounced effects of fuel oil increase occurs at the highest peaking load factor. This can be deduced from the slopes of the different curves in Figures 1-11 and 1-12, which can be represented as sensitivity values. These values reflect the increment in break-even capital cost per unit change in distillate fuel oil price. As straight line break-even capital cost curves are obtained, the sensitivity values can be regarded as valid for interpolation purposes with the distillate fuel oil price range of $\$1/10^6$ Btu to $\$4/10^6$ Btu. This range (hopefully) encompasses all expected future variations of distillate fuel oil prices. The sensitivity figures calculated here are $\$35/kW(e)$ per change of $\$1.0/10^6$ Btu for 0.05 peaking load factor operation, $\$65/kW(e)$ per change of $\$1.0/10^6$ Btu, for 0.10 peaking load factor operation and $\$145/kW(e)$ per change of $\$1.0/10^6$ Btu at the 0.20 load factor.

The black-box storage device was considered as either a peaking power plant or as a dispersed storage device, supplying both intermediate plus peak loads and designated I + P for short. In the I + P generation mode the storage device operates at an intermediate load factor of 0.5 and three peak load factors of 0.05, 0.10, and 0.20. Thus, a composite load factor can be calculated, and is a function of the distribution of the demand between the various peaking loads.

If we define f_i where i = 1, 2, 3 as the fraction of the peak demand, generated at load factors of 0.05, 0.10, and 0.20 respectively, the composite load factor (CLF) can then be calculated. Under the nominal peak load structure reported above, i.e., $f_1 = 0.125$, $f_2 = 0.375$, $f_3 = 0.500$, the CLF is found to be 0.383.

The break-even capital costs for storage devices operating at I + P loads are shown in Figure 1-13 as a function of the storage conversion efficiency, for the three distillate fuel oil prices considered. The capital costs calculated in this case can be compared with the break-even capital costs for storage devices, which apply only for peak loads. The basic feature of this comparison is that operating the storage devices to supply I + P loads is less economical than storage operation at peaking loads only. The break-even capital costs for I + P operation are lower than the capital costs for peaking devices operating at the 0.20 load factor. Operation at a composite load factor of 0.383 results in a lower allowed capital cost than operation at peaking load factors of 0.10 and 0.05, depending on the conversion efficiency and distillate fuel oil price. These basic results can be reiterated as follows:

1. Operation to supply I + P loads requires the construction of large storage plants operated on a weekly cycle. Operation to supply only the peak demand requires smaller sized plants having lower capital costs, which would be designed to operate on a daily cycle. Thus, it is more expensive to utilize storage devices for I + P mode of operation than for peaking applications only.

2. Storage devices operating at intermediate loads compete with a mix of relatively cheap direct

generation power plants which include a significant nuclear component, e.g., HTGR's. When storage devices supply peak demands they compete with gas turbines peaking hydro and pumped storage plants which have relatively higher power production costs. In order to maintain competitiveness, the break-even capital costs for I + P operation have to be lower than the allowed capital costs for peak generation only.

3. Electric storage devices incur electric-to-electric conversion losses, which effectively raise the cost of power produced by these plants. Thus, the cost of power produced by a pumped storage plant operated at a 0.75 conversion efficiency is at least 33 percent higher than the cost of off-peak power supplied to the plant. The available off-peak power is produced primarily by intermediate load plants. When corrected for conversion losses the cost of power produced by an I + P type storage device, will always be larger than the cost of directly generated intermediate load power. Therefore, in order to compete against direct generation, intermediate load plants, the break-even capital cost of the storage device has to be lower than the capital cost of the corresponding direct generation plant. This limitation does not apply when considering the application of storage devices to supply peaking loads only. The effective cost of power supplied by intermediate load plants, when corrected for conversion losses, can still be less expensive than the fuel cost of the competing gas turbines. Thus, relatively higher break-even capital costs are allowed for storage plants which supply peak demands.

The relative economic disadvantage of introducing storage devices to supply I + P loads, compared with peaking operation only results in a larger sensitivity of the break-even capital cost to variations in overall conversion efficiency. Where peaking storage plants are not at all attractive below conversion efficiencies of 0.15 - 0.20, I + P storage plants are only competitive above conversion efficiencies of 0.45 - 0.50. The conversion efficiency related component of the break-even

capital cost is the dominant cost component over the entire range of feasible efficiencies. There exists an increasing economic incentive for improving the conversion efficiency of the I + P storage plants, all the way to the maximum value of 1.0. No capital cost saturation effects, as found for operation at the 0.05 and 0.10 peaking load factors, are evident in the I + P storage plant cost computations.

As can be seen from the above discussion, it is quite conceivable that storage devices operating at relatively high conversion efficiency, and at a low load factor, will have the same break-even capital costs as storage plants operating at low efficiencies, but at higher peaking load factors. It is possible to identify bands of performance characteristics that will yield similar capital costs. The break-even capital costs calculated in this report can be utilized to specify the type of electric storage devices that will just fit the specific requirements of electric utilities. Thus, assuming a permissible capital cost figure is obtained from an electric utility production costing program, and the load factor at which the storage device is expected to operate can be specified, it is then possible to calculate the required conversion efficiency. Conversely, given the efficiency and capital cost of an existing storage device, it is possible to calculate the optimal load factor to operate that device. It is possible to assume that an electric utilities production program will assign one possible value or a narrow band of values for the allowed capital cost of electric storage plants. In such a case, a mix of electric storage plants can be implemented within the utility network to generate power at the various load factors. Smaller, but highly efficient storage plants can be utilized to generate power at the lowest peaking load factors such as 0.05. The larger and less efficient storage units will be assigned for operation at the largest peaking load factors encountered by the utility, such as 0.20. In both cases, the storage device capital cost can be very similar.

Several general conclusions can be drawn from the results of the electric storage devices break-even capital cost study discussed here:

1. Electric storage devices are best utilized as peaking devices operating at all the possible peaking load factors. Operation at both intermediate plus peaking load factors is not as economical as peaking generation only.

2. When operating as peaking plants, electric storage devices will be most economical when assigned to deliver energy at the highest poaking load factor possible. Thus, depending on the distillate fuel oil price, the break-even capital costs at 0.05 load factor vary between $250/kW(e) and $350/kW(e). When operating at 0.10 peaking load factor, the spread in break-even costs is between $300/kW(e) and $530/kW(e). The corresponding figures for operation at the 0.20 (largest) peaking load factor vary between $310/kW(e) and $750/kW(e).

3. Increasing the cost of distillate fuel oil supplied to the national energy system and burned by gas turbines within the electric sector, tends to increase the break-even capital costs of the electric storage devices. The increase in capital costs is more pronounced as the electric storage devices are assigned to higher load factor peaking operation.

4. Improving the electric-to-electric overall conversion efficiency of the storage plants will greatly increase the allowed storage capital costs in the efficiency range of 0.25 to 0.55. A more moderate effect on increasing capital costs can be attributed to improving the conversion efficiency in the range of 0.55 to 0.80. Above an efficiency value of 0.80 there is little economic incentive measured in increasing capital costs per unit efficiency improvements.

5. When meeting peaking demands at different load factors, a mix of storage devices with different performance characteristics may be desirable. Highly efficient storage devices can be assigned

to meet the demand at the lowest load factor (0.05). Larger and less efficient storage plants (efficiency range of 0.55 - 0.65) can still be economic when assigned to peaking load generation at the relatively higher load factors of 0.10 and 0.20. The exact nature of an optimal storage plant mix can only be determined in a detailed storage implementation study, taking into account full range of characteristics available from the various storage devices that may be produced from current research and development efforts.

PROGRESS IN AREA 2: HYDROGEN PRODUCTION AND AUXILIARIES

Task Group 2.1 Test Devices

Scope: Examine the chemistry, physics, and materials problems associated with advanced electrolytic concepts including low temperature ($<100^{o}C$) aqueous, high-temperature fused salt, and solid electrolyte systems. This activity involves a review of the past development efforts of other investigators in light of recent developments and improvements in materials. The emphasis will be on the development of high performance systems, the ultimate goal being electric-to-hydrogen conversion efficiencies exceeding 90% (voltage efficiency) and installed capital costs below $50/kW thermal hydrogen output.

An effort will be made to continuously review progress in the development of other production methods, e.g., thermochemical and biological.

Progress During the Report Period: Evaluation of General Electric Solid Polymer Electrolyte Water Electrolysis Cell Including Temperature Effects: The following experiments were carried out in order to obtain a more detailed evaluation of this water electrolysis concept:

(i) Independent cell potential--current density measurement to check the reproducibility of the cell at $25^{o}C$.

(ii) Effect of electrolysis at a current density of 120 ASF ($\sim$120 ma cm^{-2}) for varying times on the performance characersitics of the cell at $25^{o}C$.

(iii) Effect of temperature (from 25^{o} to $82^{o}C$) on the cell potential--current density relations.

(iv) Cell potential--current density relations on individual cells in 3 cell stack at $25^{o}C$.

From these studies, it was concluded that (i) the results of three independent experiments showed good reproducibility

in cell potential--current density relations; (ii) continuous operation of the cell at a current density of 120 ma cm^{-2} for 16 hours or 46 hours did not alter the performance characteristics of the cell; (iii) increase of temperature produces a significant improvement in cell performance. At a temperature of about 80°C and a current density of 200 ma cm^{-2}, the GE cell has a voltage efficiency of about 95%; and (iv) the 3 cells in the stack behaved very similarly.

To further improve the performance of the GE cell, it is necessary to use thinner electrolyte layers (e.g., 6 mils instead of 12 mils) and to reduce the overpotential at the oxygen electrode by the use of alternate catalysts. Though noble metal catalysts are used in this cell, there is a high degree of utilization of catalyst particles in the cell. According to the configuration of the cell, it may be possible to reduce catalyst loadings to such levels that the catalyst cost or availability will not be the limiting factors in the development of the cell.

Further details of the above studies on the General Electric cell are found in a Quarterly Report[1] and in a recent publication.[2]

Effect of Temperature on the Performance of Teledyne Alkaline Water Electrolysis Cell: The Teledyne cell was tested with 30% KOH as the electrolyte at three temperatures (25°, 65°, and 82°C) under conditions of higher electrolyte pumping rates and over a considerably longer range in current density (20 to 1100 ASF) than done previously. Activation overpotentials at both the hydrogen and oxygen electrodes contribute significantly to the efficiency losses in this cell at current densities below 400 ma cm^{-2}. Ohmic overpotential effects are predominant above this current density. At a current density of 600 ma cm^{-2}, the cell potential and voltage efficiency are 2.2 volts and 68% respectively (cell temperature 82°C).

The present results at a temperature of 82° and in the current density range from 100 to 500 ASF are in agreement with those obtained previously. Attempts made to determine the ohmic drop in the cell by the current interruptor method were unsuccessful, probably due to the large capacitance

component. Upon careful removal of one of the cells in the 5 cell module, it was found that its construction was non-uniform--the anode side had 2-20 mesh nickel screens while the cathode side used a nickel screen for the electrode and expanded metal for the electrolyte gas flow.

The results of temperature effect on the performance of the Teledyne cell are found in a Quarterly Report[1] and a recent publication.[2]

Effect of Temperature for Hydrogen and Oxygen Evolution Reactions on Nickel Electrodes in KOH Solutions: It is essential to attain nearly a 100% voltage efficiency (efficiency based on ΔH value) in water electrolysis cells for hydrogen production by this method to be economically competitive with conventional methods of hydrogen production from fossil fuels (e.g., from coal or natural gas). Most commercial water electrolyzers operate at 70°to 90°C in alkaline solution with nickel or stainless steel electrodes at voltage efficiencies of 65 to 75%. Activation overpotentials at the hydrogen and oxygen electrodes are the major contributions to the efficiency losses in water electrolysis cells.

The purpose of the present study was to ascertain the advantages of higher operating temperatures for water electrolysis in 50% potassium hydroxide solution using nickel electrodes. Tafel slopes, transfer coefficients and exchange current densities were determined for both the hydrogen and oxygen evolution reactions at temperatures of 80°, 150°, 208° and 264°C.[3] The experiments were conducted in a stainless steel pressure vessel. A dynamic hydrogen electrode, as described by Giner,[4] was used as the reference electrode. Investigations of the hydrogen and oxygen evolution reactions were made by simultaneously recording the current potential relations at the cathode and anode respectively in stirred KOH solution contained in a three-compartment Teflon cell. Smooth nickel disks of geometric area 0.2 cm^2 were used as the electrodes. The electrochemical measurements were made using a PAR model 173 potentiostat with a PAR Model 175 programmer. Current potential relations were determined by using a slow potential sweep (sweep rate 1 mv/sec) and by steady state potentiostatic measurements. The measurements were always made in the direction of high to low currents and returning to high currents.

Figure 2-1 shows the average results from four independent experiments for the hydrogen and oxygen evolution reactions at temperatures of 80°, 150°, 208°, and 264°C. Distinct linear Tafel regions were observed at each temperature for both the hydrogen and oxygen evolution reactions. As seen in Figure 2-1, each study of the oxygen evolution reaction at 208°C indicated the existence of dual Tafel regions. The electrode kinetic parameters (Tafel slope b, transfer coefficient α and exchange current density i_o) for the hydrogen and oxygen evolution reactions, as a function of temperature, are presented in Table 2-1. The exchange current density (i_o) for the hydrogen evolution reaction (HER) increases from 1.1×10^{-4} at 80° to 10^{-3} amp cm^{-2} at 264° while i_o for the oxygen evolution reaction (OER) increases from 4.2×10^{-6} at 80° to 10^{-3} amp cm^{-2} at 264° C. The transfer coefficient for the hydrogen evolution reaction was approximately 0.5 in this temperature range while for the oxygen evolution reaction changed from 0.7 to 3.3. Due to the marked enhancement of reaction kinetics for the oxygen evolution reaction at higher temperature, which was also associated with a marked decrease of Tafel slope, voltage efficiencies approaching 100% for water electrolysis can be attained at about 150°C in the current density range from 200-400 ma cm^{-2} (one must take into consideration that smooth wire electrodes with a low roughness factor were used in the present investigations). Asbestos, which is used as the separator material in most of the commercial water electrolyzers, disintegrates in a KOH environment at temperatures above 100°C. It will therefore be necessary to replace asbestos with a more stable separator material for attaining nearly a 100% voltage efficiency in water electrolysis cells with nickel electrodes operating at a temperature of 150°C.

A Dynamic Hydrogen Electrode for Hydrogen and Oxygen Overpotential Measurements at Temperatures above 100°C: Commercial reference electrodes such as calomel, mercury-mercuric oxide, silver-silver chloride, etc. have temperature limitations. At present, the commercially available electrodes can withstand temperature only as high as 130°C.[4] Since these electrodes are not suitable for the study of the electrocatalytic activities of Ni for the hydrogen and oxygen evolution reactions at intermediate temperature (80-264°C), a dynamic hydrogen electrode (DHE) originated by J. Giner[5] was selected as the reference electrode. The potential of DHE should be

reasonably stable so that any inaccuracy in the overpotential measurement must not be attributable to this reference electrode. In this study, the stability of the potential DHE was first investigated in concentrated alkaline solution at room temperature. In order that the exchange current densities of the hydrogen and oxygen electrode reactions can be accurately determined, the overpotential of DHE, i.e., the potential difference between DHE and RHE (the reversible hydrogen electrode) in the same solution, was also ascertained in the temperature range of 25° - 264°C.

In the experimental procedure a platinum foil of .1 cm^2 surface area was connected, by spot welding, to a platinum wire of 30 mils in diameter, which was sealed in a shrinkable Teflon tubing. Then, this platinum electrode was treated, cleaned and finally platinized in chloroplatinic acid solution by following the procedures described in the monograph edited by Ives and Janz.[6] A schematic arrangement of the three compartment cell used in this work is shown in Figure 2-2.

When the measurements were made in the glass beaker-type cell, it was found that the potential difference between DHE and RHE was quite unstable. After 1 hour of equilibration, the rate of change of the potential of RHE/DHE is larger than 0.25 mv/min.[7] The instability of the RHE/DHE potential encountered in this case was attributed to (1) the long time required to saturate the large amount of measuring solution (250 ml) with H_2; (2) the contamination of electrode surface caused by the attack of glass cell by the concentrated (50 wt.%) KOH solution; and (3) the diffusion of O_2 from the auxiliary electrode, which works as the oxygen evolving electrode, to the DHE (this causes the potential of RHE/DHE to become higher).

The use of the Teflon cell with a small compartment (less than 10 ml) to contain both DHE and RHE, can essentially eliminate the disadvantages mentioned above. However, when the measurements were carried out in the three-compartment Teflon cell, the shift rate of RHE/DHE potential was found to be as large as 0.10 mv/min. after one hour of equilibration.[7] This phenomenon could be attributable to the unstable potential of the RHE and/or the DHE. Thus, using a saturated calomel electrode (SCE) as the reference, the time

dependence of the RHE and of the DHE in 50 wt.% KOH solutions at 25°C was measured independently. As shown in Figure 2-3 the shift rates of the potentials of RHE and of DHE are quite large (0.64 and 0.37 mv/min. respectively) after 10 minutes of equilibration. After 30 minutes, the potential of DHE is practically stabilized (changes of less than 1 mv in 100 min.), however, the rate of change of the RHE potential is still as large as 0.1 mv/min.

In the study of the DHE/RHE potential in 50 wt.$ KOH solution as a function of temperature, two independent runs starting from room temperature (23°C) were performed. After bubbling H_2 overnight at room temperature, the potential difference between the DHE and RHE was always found to be about 60 mv. As shown in Figure 2-4 the reproducibility of the DHE/RHE potential vs. temperature plots is reasonably good. As the temperature of the electrolyte was increased, the potential difference of DHE/RHE was slightly reduced until a value of ~35 mv was attained at 264°C.

In this study, it is concluded that (1) after 30 minutes of equilibration at 1 mA/cm^2, the potential of DHE is practically steady enough to be used as a reference electrode; (2) the unstable potential of RHE could be attributable to the intrinsic impurities from the KOH solution which contaminate the electrode surface and thus reduce its activity; and (3) similar to the observations by Giner, the overpotential of the DHE in KOH solutions reduces only slightly with increasing temperature. A convenient reference electrode is now available for practical measurements on various anode or cathode assemblies for use in water electrolysis systems.

Selection and Evaluation of Separator Materials for Water Electrolysis Cells: Higher operating temperatures are necessary to approach 100% efficiency in water electrolysis cells. To develop an alkaline water electrolysis cell operating at about 150°C, it is essential to find a replacement for asbestos, which is the separator material in current use.

An evaluation of Teflon and several other materials for fabrication of cell electrolysis barriers was carried out, and some of the more promising materials are Betalux 201 R, Kynar, polypropylene, and polysulfone. Kel-F was found to be a very satisfactory material, but is expensive.

During the year, several materals were selected and tested as barrier materials in water electrolysis cells. The electrode assemblies were changed from those which required several days to machine using solid nickel to the present configuration made from two pieces of 20 mesh nickel screen and then pressed on a die to give the proper shape. With this type of assembly, it is possible to test six materials with the cells connected in series thereby assuming a constant current density on all materials under test. It was also found necessary to use the same electrodes as anodes and cathodes each time due to the change in the composition of the nickel anode during the test run. Of the materials tested to date, the most promising are potassium titanate and permion 1010. As far as electrical resistance is concerned, some of the non-woven polypropylenes look promising, although they are restricted to a maximum usable temperature of 135°C. Gas permeability has not been determined. Many more materials which have been received, will be tested during the next year. All materials are currently tested at 25°, 40-60° and 85-100°C. The most promising ones will then be tested at 135° to 150°C. Preliminary results were presented in a recent publication.(2)

Automation of Oxygen Overpotential Measurements: In the electrochemical studies, conventional steady state potentiostatic or galvanostatic measurements to obtain Tafel plots are accurate but time consuming. For example, in a potential range of 1 volt in which the electrochemical activities of an electrode are investigated using the steady state potentiostatic method, it takes at least 4 hours to obtain a Tafel plot, including measurements, calculation and plotting. In order that the electrocatalytic properties of electrode materials for water electrolysis can be determined accurately, efficiently, and above all rapidly, an alternative technique for evaluating electrocatalysts was developed and tested.

By connecting a log converter to the potentiostat and varying the potential of the test electrode linearly with time, using a signal generator, the Tafel plots can be recorded directly on an X-Y recorder. Comparing with the steady state potentiostatic measurements, this transient technique (using sweep rate of 0.1, 1, 5 and 10 mv/sec) was employed to determine the Tafel parameters for the oxygen evolution reaction on nickel and Ni_3Ti (an intermetallic compound) in 30% KOH solution at 80°C.

A potentiostat (PAR Model 173) coupled with a log converter (PAR Model 376) was used to make the electrochemical measurements. In the transient technique, a programmer (PAR Model 175) was also connected to the potentiostat. The "log I output" signals from the log converter were connected to the X-Y recorder so that the Tafel plots were recorded directly on the semi-logarithmic papers. On the other hand, the "I output" of the log converter was connected to the strip chart recorder to check simultaneously the current appearing on the X-Y recorder.

For the oxygen evolution reactions on Ni_3Ti electrode in 30% KOH solutions at 80°C, two independent steady state potentiostatic and one transient measurements at the sweep rate of 0.1 mv/sec were carried out using different solutions and electrode settings in the potential range of 0.15 - 0.6 volt vs. SCE. For the nickel electrode, all the electrochemical measurements using steady state potentionstatic method and transient technique at various sweep rates (0.1, 1, 5, and 10 mv/sec) were made under the same experimental conditions in the potential range of 0.15 - 0.95 volt vs. SCE. In both steady state and transient measurements, the Tafel plots were always determined in the direction of high currents to low currents and then reversed.

The original Tafel plot using transient technique at a sweep rate of 0.1 mv/sec in both cathodically and anodically scanning directions for the oxygen evolution reaction on Ni_3Ti is shown in Figure 2-5. The Tafel plots from two independent steady state potentiostatic measurements which are also plotted in the same figure give equal Tafel slopes of 0.087 volts and very close exchange current densities (4.8×10^{-6} and 6.0×10^{-6} A/cm^2, respectively). On the other hand, transient measurements provide a lower Tafel slope (0.078 volts) and lower exchange current density (3.0×10^{-6} A/cm^2). This is probably attributed to the fact that a relatively thinner oxide film is formed on electrode surface by using transient techniques. Because of different experimental conditions of these three independent measurements, the Tafel plots show a maximum shift of about 30 mv in the linear region as seen from Figure 2-5.

For the oxygen evolution reactions on nickel electrode in 30% KOH solution at 80°C, the electrochemical measurements

were carried out using both steady state potentiostatic and transient techniques based on the same experimental conditions. By taking the average value of the cathodic and anodic scannings, the Tafel plots at various sweep rates are presented in Figure 2-6. Using the same solution and electrode setting, the data from steady state measurements are also shown in this figure (open circles).

The Tafel slopes, the transfer coefficients, the exchange current densities and the experimental order for the various measurements at different sweep rates are shown in Figure 2-6. A freshly prepared nickel electrode is first studied using transient technique at a sweep rate of 1 mv/sec. When the second measurement is performed at a sweep rate of 0.1 mv/sec, the Tafel plot goes down about 20 mv in the linear region. At the current density less than 100 mA/cm^2, these two Tafel plots are almost parallel to each other. As seen from Figure 2-6, when more experiments are carried out on the same Ni electrode at sweep rate 5 mv/sec, then 10 mv/sec, and finally by steady state method, the Tafel lines are parallel. From these observations, it is concluded that the position of Tafel plot is correlated with the history of the test electrode. Since the exchange current densities are strongly dependent on the position of Tafel plots, they do not provide correct information to judge whether the transient technique can be used to replace the steady state potentiostatic measurements. However, as seen from the third column in Figure 2-6, the Tafel slope decreases with increasing the sweep rate. The transient measurements at a sweep rate not more than 5 mv/sec provide Tafel parameters very similar to those from steady state potentiostatic measurements. However, at the sweep rate of 0.1 mv/sec, it takes even longer time than that required by using steady state method for the range of potential to be studied.

After treating an electrode at a higher current density to form a sufficiently stable oxide film on its surface, the transient technique at a sweep rate of 1 - 5 mv/sec provides an efficient, accurate and time-saving method for the evaluation of electrocatalytic activities of electrode materials for oxygen evolution reactions. At a sweep rate of 1 mv/sec, the transient technique coupled with a log converter and an X-Y recorder takes about one-fifth of the time required to obtain a Tafel plot using steady state potentiostatic method in the same range of potential involved.

Investigation of Electrocatalysts for Alkaline Water Electrolysis Cells:
Nickel Based Alloys

In addition to nickel as the electrode material for the evolution of oxygen in KOH solutions, various alloys were also examined.[8] Table 2-2 indicates that catalytic properties can be favorably modified by combining the proper elements. Each compound listed consists of elements neighboring on each side of a good catalyst in the periodic table, and each is better than the individual elements as electrocatalyst for the hydrogen evolution reaction. However, only TiCu would be stable enough in alkaline solutions for use as a catalyst for the oxygen evolution reaction.

The changes in electrocatalytic properties of alloys have been reported to parallel changes in the number of d-band vacancies.[9] Each nickel atom possesses two d-band vacancies. Alloying nickel with other transition elements with partly filled d-shells produces more d-band vacancies in nickel and thus it is possible to deduce its influence on the electrocatalytic properties. The electrochemical performances of three nickel-titanium intermetallic compounds, i.e., Ni_3Ti, NiTi, $NiTi_2$, were carried out at 80°C in 30% KOH solutions contained in the Teflon cell. Tafel slopes, transfer coefficients, and exchange current densities were determined from the potential vs. current density relations for the oxygen evolution reaction and are shown in Figure 2-7.

The introduction of Ti possessing partly filled d-shells into nickel should increase the number of d-band vacancies and hence enhance its electrocatalytic activity. This was confirmed in the case of Ni_3Ti which appears to be a better electrocatalyst than pure nickel for oxygen evolution reaction in the alkaline systems. However, titanium oxide, formed during oxygen evolution, is an insulator and eventually, when present in large amounts, it will reduce the electrocatalytic activity of NiTi alloys. The electrochemical behavior of NiTi nearly resembles that of Ni, while $NiTi_2$ appears to be a poor electrocatalyst with limiting current of approximately 55 mA/cm^2.

A similar study on some other nickel alloys is summarized in Table 2-3. When compared with the electrochemical behavior of pure nickel, none of these alloys showed any improvement in exchange current density.

Oxygen Evolution Reaction on Spinels

Mixed oxides are known to be good electrocatalysts for oxygen evolution.[10] Some spinels, particularly $NiCo_2O_4$, have shown promise as good electrocatalysts for oxygen reduction.[11] We have examined $NiCo_2O_4$ as anode material for oxygen evolution. Preliminary results show this substance to be no better than nickel in alkaline solutions.

In preparing $NiCo_2O_4$, two nitrates, $Ni(NO_3)_2.6\ H_2O$ and $Co(NO_3)_2.6\ H_2O$, were weighed in the exact proportion of Ni:Co, 1:2 and dissolved in water. The solution was evaporated to dryness until there were no more NO_2 fumes. The black powder was now heated in an electric furnace in air for 48 hours at a temperature of 325-350°C. For further details, Reference 12 can be consulted.

All electrochemical studies on $NiCo_2O_4$ were done in 30% KOH at 80°C. Steady state potentiostatic technique was used. The spinel, $NiCo_2O_4$ were in a proportion of approximately 20:80 by weight. A nickel screen was dipped in the above solution and a coating of $NiCo_2O_4$ was deposited on it. The nickel screen was heated in an electric furnace for about an hour at 310°C. The electrode so prepared was used as an anode for oxygen evolution.

The results are shown in Figure 2-8. From these results it appears that $NiCo_2O_4$ is comparable to nickel for the oxygen evolution in 30% KOH solution but no better. The Tafel slope, transfer coefficient, and exchange current density are given in Figure 2-8.

There were many problems with using $NiCo_2O_4$ as electrode material in the above manner. Binding of $NiCo_2O_4$ to substrate, such as nickel screen, is not easy. Teflon may increase the resistance of the material very much thus decreasing its electrocatalytic activity. To avoid this, $NiCo_2O_4$ was prepared

on the substrate by thermal deposition. Work with such electrodes is underway in our laboratory. They appear to be much better than Teflon-bonded electrodes.

Investigation of Electrocatalysts for Acid Water Electrolysis Cells*

Most commercial water electrolyzers operate at 70° to 90°C in 25-35% potassium hydroxide solutions using nickel electrodes. A possible improvement in water electrolysis as a route for hydrogen production is the use of solid polymer electrolytes such as General Electric's perfluorinated sulfonic acid polymer. In a hydrogen energy storage system for electric utility operations, it is economically advantageous if a single unit can serve both as a water electrolyzer and as a fuel cell. During electrolysis, the hydrogen ions produced by the oxidation of water move across the solid polymer electrolyte and are reduced to form hydrogen at the cathode. One disadvantage of such a system is the acid environment which develops at the anode causing corrosion of metals such as nickel. In this study, various metals are investigated for possible use as electrocatalysts for water electrolysis in an acid medium at 80°C. Correlations between the observed overvoltages and metallic properties are discussed. A previous study in alkaline solutions has shown that cyclic voltammetry is a convenient method for evaluating electrocatalysts for water electrolysis.[8]

The method used to evaluate the various metals as electrocatalysts was cyclic voltammetry using a potential sweep rate of 50 mv/sec. Details of this method are reported elsewhere.[8] For Pt, Ir, and RuO_2, potentiostatic steady state studies were made to determine Tafel parameters and the exchange current densities. The ruthenium and osmium electrodes were notably different from the others since they were formed by electroplating the metal onto a platinum wire electrode. A ruthenium oxide electrode formed on titanium similar to those used in the chlor-alkali industry[13] was also tested.

The cyclic voltammetric traces for the iridium electrode in 0.1M H_2SO_4 at 80°C are shown in Figure 2-9. The horizontal line segments show where the current attains a value of 2mA/cm^2 based on the geometrical area of the electrode.

*Research carried out by Dr. M. H. Miles, M. A. Thomason, J. R. Locker, and W. E. Serafin at Middle Tennessee State University under BNL subcontract No. 347505S.

From the Tafel equation

$$\eta = a + b \log i, \qquad (1)$$

the experimental overvoltages for hydrogen or oxygen evolution at 2 mA/cm^2 for the various metals should reflect changes in the Tafel parameter, a, and hence changes in the exchange current density, $i_o = 10^{-a/b}$, as long as the Tafel slope, b, remains constant for a given reaction on various metals.

Figure 2-10 presents a summary of all cyclic voltammetric results on various metals in 0.1M H_2SO_4 at 80°C. The solid circles at the negative potentials locate hydrogen evolution at 2 mA/cm^2 while the solid circles at the positive potentials locate oxygen evolution at this current density. The open circles show the potentials at which the current density exceeds 2 mA/cm^2 due to some other anodic process such as oxidation of the metal. For Cr, Mn and Fe, hydrogen evolution and anodic oxidation are observed at about the same potential. The potentials for Ti, Zr, Hf, Ta, and Pd were not as reproducible as those for other metals. This is likely due to hydride formation which changes the surface properties. For hafnium, the anodic limit observed at about -0.2 V probably results from oxidation of the metallic hydride. No reproducible anodic limits were observed for Ti, Zr, and Ta. Although oxygen evolution was initially possible, these surfaces soon passivate due to formation of insulating oxide films.

Figure 2-11 presents results for potentiostatic, steady state studies of oxygen evolution on Pt, Ir, and RuO_2 in 1.0M H_2SO_4 at 80°C. The potential required for a current of 2 mA/cm^2 is about 0.3V less on Ir than on Pt, which is in excellent agreement with the corresponding results in Figure 2-10. It is difficult to compare RuO_2 with Ir due to the much higher surface roughness factor for RuO_2. However, a stable electrode with a high roughness factor is a desirable property for water electrolysis. Judging from Figure 2-11, the catalytic activities for Ir and RuO_2 would be about equal if the surface roughness factor for RuO_2 is about 50-100 times larger than that for Ir.

Periodic variations of hydrogen overvoltages with atomic numbers of the electrode metals are evident from Figure 2-10. The overvoltages show minima for Ni, Pd, and Pt which have d^8s^2, $d^{10}s^0$, and d^9s^1 electronic configurations, respectively. Large hydrogen overvoltages are observed for Zn, Cd, and Hg which are all of the $d^{10}s^2$ electronic configurations. The periodic trends observed for hydrogen overvoltages in acid solution show a high correlation with the work function of the elemental metals. Using the same work function values adopted by Trasatti,[14] the location of the experimental potential, E, versus SCE at $2mA/cm^2$ for the transition metals is given by

$$E = 0.64\phi - 3.5, \qquad (2)$$

where ϕ is the work function in electron volts. Figure 2-12 shows the E vs. ϕ plots for both transition metals and sp metals. The correlation coefficient for the least square fit for the transition metals is 0.88 suggesting a high correlation between the observed hydrogen overvoltage and the work function. For the non-transition metals tested, the correlation between the observed hydrogen overvoltage and the work function is much less precise since the calculated correlation coefficient is only 0.29. The overvoltages on Zn, Cd, Hg, and Pb actually seem to be nearly independent of the work function. The heat of adsorption of hydrogen on metals is theoretically related to the rate of electrolytic hydrogen evolution[15,16] and experimental correlations have been observed (5). Figure 2-13 shows the plot of the potential observed at 2 mA/cm^2 against the M-H bond strength of the metal as derived by Krishtalik[16] from experimental data for hydrogen evolution. The predicted volcano-shaped curve is obtained and looks similar to results based on i_o values.[14] Figure 2-13 suggests the presence of a horizontal region where the overvoltage remains small for M-H bond strengths between 52-60 kcal/mole. Such horizontal regions are predicted when the adsorption equilibrium follows a Temkin isotherm.[15]

In general, the overvoltage required for the discharge of hydrogen ions onto a metallic surface

$$M + H^+ + e^- \rightleftarrows M\text{-}H \qquad (3)$$

decreases with increasing M-H bond strength while the overvoltage required for removing the adsorbed hydrogen atoms

$$M\text{-}H + H^+ + e^- \rightleftarrows M + H_2, \qquad (4)$$

or

$$M\text{-}H + M\text{-}H \rightleftarrows M + H_2 \qquad (5)$$

increases with increasing M-H bond strength. Thus, for metals in Figure 2-13, where the M-H bond strength is less than about 50 kcal/mole, the discharge step in equation (3) is usually rate-determining. For metals where the M-H bond strength is greater than about 60 kcal/mole, either slow electrochemical desorption as in equation (4), or slow recombination as in equation (5) controls the reaction rate. However, such mechanism assignments are somewhat ambiguous since volcano curves are predicted for each mechanism.[15,16] The only large discrepancies between Krishtalik's values for the M-H bond strength and adsorption data from the gas phase are found for Fe, Co, and Ni. Krishtalik's value of about 46 kcal/mole is based upon the assumption of a slow discharge step on these metals in acid solution,[16] however, measurements of hydrogen-tritium separation factors on nickel and iron indicate a slow electrochemical desorption step at high overvoltages.[17,18] Perhaps the low coverage of hydrogen on these metals places them on the other branch of the volcano curve for the electrochemical desorption mechanism.

The best electrocatalysts for the hydrogen evolution reaction in 0.1 M H_2SO_4 at 80°C are found to be in the order Pd>Pt≈Rh>Ir>Re>Os≈Ru>Ni. For the ruthenium and osmium electrodes, a roughness factor of about 20 relative to the other metals, was assumed. Judging from Figures 2-10, 2-12, and 2-13, an ideal electrocatalyst lacks two electrons in filling its outermost d and s sublevels, has a work function of about 5 eV, and forms M-H bonds with energies of about 52-60 kcal/mole.

For the oxygen evolution reaction, the catalytic activity in acid solution is found to be in the order Ir≈Ru>Pd>Rh>>Pt>>Au>>Nb. Nearly all other metals either undergo anodic corrosion or form passivating oxide films in 0.1 M H_2SO_4 at 80°C, hence the choice for elemental metals as useful catalysts for the

oxygen evolution reaction in acid solutions is limited to the precious noble metals. Based upon the cyclic voltammetric and steady state results, iridium and ruthenium appear to be the best electrocatalysts for oxygen evolution in acid solutions. Both form oxides (IrO_2, RuO_2) having high electronic conductivities[19] which promotes the electron transfer through the oxide layer. Results for ruthenium plated onto platinum and for ruthenium oxide electrode were similar, except that the ruthenium plated electrode gradually disintegrated during oxygen evolution while the mixed oxide of RuO_2 and TiO_2 on titanium was stable.

Tafel parameters calculated for the oxygen evolution reaction on Pt, Ir, and RuO_2 in 1.0 M H_2SO_4 at 80°C are given in Table 2-4. The smaller Tafel slope observed for RuO_2 is an attractive advantage for this material. Overvoltages for oxygen evolution at 20 mA/cm^2 and 200 mA/cm^2 are given in Table 2-5. Even at current densities typically used for water electrolysis, the overvoltage on Ir in acid solution is about 0.3V less than that observed on Pt. The smallest overvoltage based on geometrical electode areas are observed for RuO_2. Considering the large roughness factor and small Tafel slope, the mixed oxide of RuO_2 and TiO_2 appears to be the best electrocatalyst for oxygen evolution from acid solutions.

Design and Fabrication of Two Cell Bipolar Water Electrolyzer

For membrane barrier testing and observation purposes, a two cell bipolar water electrolyzer was constructed. Although the cells were build quite large for observation, the working electrodes were only 0.050 inch apart for barrier material evaluations. The unit is a gravity feed, i.e., the gas bubbles actually work to the pumps and circulate the electrolyte. Two separate chambers above the unit serve to collect the hydrogen and oxygen generated. Also included is a pressure equalizer loop. A lead from the bipolar plate makes it possible to study the long time effect of KOH and ion flow on two barrier materials simultaneously. At the present time an ion exchange membrane (permion 1010) is being used as the gas barrier.

Evaluation of Engelhard Hydrogen-Air Fuel Cell

During a brief period when a 750 watt fuel cell was available on loan, it was tested at different flow rates of hydrogen

from about 3 liters/min to a maximum of 15 liters/min. This unit consumed about 14 liters of hydrogen per minute when supplying 30 amps at 24-6 volts. We were satisfied with this fuel cell and have placed an order for a 50 watt unit to be used for test and evaluation.

PROGRESS IN AREA 3: HYDROGEN STORAGE DEVELOPMENT

Task Group 3.1 (a) Engineering Test Beds

Scope: Survey existing data and determine areas to be investigated. Design, construct, and operate laboratory apparatus to obtain data necessary to determine feasibility and to design test facilities (Area 5). Among the data to be obtained are (1) thermal conductivity of granular iron-titanium compounds; (2) the changes, if any in these compounds, resulting from flowing hydrogen through packed beds of granular FeTi compounds both before and after repeated hydriding/dehydriding cycles; (4) the kinetics of the hydriding and dehydriding reaction; and (5) resistance of container materials to hydrogen embrittlement or loss of ductility. It is anticipated that a number of individual test beds will be required in order to satisfy all of the data needs.

Summary of Previous Work: 10-lb Hydrogen Reservoir: In March of 1973 BNL contracted to build an engineering-scale hydrogen reservoir for Public Service Electric & Gas Company (PSE&G) of New Jersey on a cooperative financial basis. The reservoir is being used in an experimental facility which has the overall objective of demonstrating the feasibility of storing electrical energy through the production, storage, and reconversion of hydrogen. The objective is to be accomplished by producing hydrogen from a water electrolyzer (Teledyne Isotopes Corp.), storing it as iron titanium hydride, and subsequently regenerating it from the hydride to be used with air in a fuel cell (Pratt & Whitney Corp.) rated at 12.5 kW (ac). The reservoir was designed to store 10 lb of hydrogen and to be capable of handling 1.5 lb/hr. Hydrogen from the electrolyzer is pressurized to 500 psia with a diaphragm compressor (Pressure Products Industries, Inc.) in order to provide the driving force during hydriding. The hydride reaction is reversible, and the thermal load of approximately 7000 Btu/lb hydrogen can be satisfied by circulating water through the internal heat exchanger tubes. During charging of the reservoir, cold water at 50-80^{o}F is to be used; whereas for discharging hydrogen, hot water at 80-130^{o}F is to be used.

The vessel consists of a body made from 12 in. diam. pipe with end caps welded to it (6.5 ft long, 316 SS), porous-metal tubes for hydrogen collection and distribution (6 tubes parallel to and branching from the axial gas line, 316 SS), U-bend tubes for water flow (9 tubes parallel to the vessel axis, 304 SS), grid plates for supporting the porous-metal and water tubes in a fixed geometry, (4 plates held together by the rods, 304 SS) and 30 thermocouples for monitoring internal temperatures. After the vessel was fabricated and tested it was filled with 879 lb of FeTi alloy (Cannon-Muskegon Corp.) using the screened fractions ranging in size from 4 to 100 mesh. The initial step of activating the alloy, by a process of heating, evacuation and contacting with hydrogen, was done over a two-week period, during which time 14.3 lb of hydrogen had reacted to produce material equivalent to $FeTiH_{1.67}$. In the limited time available for testing prior to delivery of the reservoir to PSE&G (February 1974), it was demonstrated that the reservoir could accommodate 13 lb of available hydrogen and release it at a rate of 2.5 lb/hr. At PSE&G the reservoir was incorporated into their Hydrogen-Energy Storage Test Facility, replacing a tube trailer of pressurized hydrogen, and the first charging run was made without difficulty. An operating manual was prepared for their use.

Progress During the Report Period: 10-lb Hydrogen Reservoir: The first operations with the reservoir served mainly for the training of personnel and further checking of the energy storage system (electrolyzer, hydride reservoir, and the fuel cell). Subsequently difficulties with the electrolyzer and the fuel cell necessitated their replacement. The first complete and continuous charging run was made on August 7, 1974; 12.02 lb of hydrogen was charged over a 10-hour period. Four hours into the run, when the reservoir appeared to be in good dynamic equilibrium, its performance was compared with the design value of UA in the equation $q = UA\Delta t$. From the observed values of the Δt (26.1°F), the hydrogen flow rate (1.36 lb/hr), and the heat of association (based on 6700 Btu/lb H_2), the value of UA (349 Btu/hr °F) was calculated; this is 150% of the design value. It is interesting to note that 87% of the hydrogen was charged before the bed pressure increased to 350 psia, because this value is lower than that of commercial high-pressure electrolyzers, the use of which would eliminate the compressor.

The first 14 runs were hampered by various operating problems, including hydrogen leakage in the triple diaphragm assembly of the compressor. This failure was due to the formation of a crack in the primary diaphragm and was most likely caused by the intrusion of particulate matter in the gas stream. After installation of a thermal-type mass flowmeter for hydrogen, a formal series of runs was started. Cycles 15-22 were usually made over the course of two days for each part of the cycle; the rate on the first day was a nominal 1.4 ± 0.1 lb H_2/hr, and on the second day the average rate was usually lower because the hydride was approaching depletion or saturation. The water flowrates used were 1.5, 3.0 and 5.0 GPM and the water inlet temperatures were 52°/120°, 70°/100° and 80°/80°F for the charge and discharge portions of the cycle. The main effect of varying the water flow rate was simply one of arriving at a different water Δt. Of particular importance was the effect of using a common intermediate water temperature, 80°F, for both portions of the cycle. The principal effect of using a high inlet water temperature (80°F) during charging was to reduce the amount of hydrogen stored in the allotted time. This limitation occurs because the higher resulting association pressure decreases the driving force, which is the difference between the compressor and association pressures. Likewise, the use of a low inlet water temperature (80°F) during discharging reduced the amount of hydrogen released in the allotted time because of the lower dissociation pressure and the desire to keep the reservoir at essentially the same terminal pressure--which is no lower than 30 psia.

There was an apparent error in the hydrogen inventory during the course of these cycles because at one point the reservoir stored more hydrogen than expected. Prior to the start of cycle 15 the bed was exhausted to about 1.13 lb of residual hydrogen, which is unavailable under normal operating conditions; thus at the start of cycle 15 the amount of available hydrogen was considered to be zero. Subsequently the inventory consisted of summing up the integrated flows obtained from the mass flowmeter. At one point the amount of available hydrogen was 15.6 lb, or 1.3 lb in excess of that determined at BNL. This high amount of available hydrogen plus the residual amount equals an apparent total of 16.73 lb and corresponds with the hydride composition $FeTiH_{1.96}$ at that time. A value of H this high is considered unlikely because of the lower purity of the commercial grade of FeTi used; rather it appears that the integrated hydrogen flow is high by about 15%.

Summary of Previous Work: Small-Scale Test Beds: Design work was started on two test beds which use different methods of handling the thermal load in a hydride reservoir. The first bed, a convection-type designated B-1, utilizes circulating hydrogen gas as the heat transport medium; its requirements are such that about 2% of the flow is for process use and the remainder is necessary thermally. Thus a high-capacity compressor is required along with an external hydrogen/water heat exchanger. The use of an existing diaphragm compressor (being modified) limited the present vessel size to 1.5-in. pipe, 1.5 ft. long. The second test bed, a conduction type designated B-2, utilizes circulating water in a jacket to handle the thermal load; the design and construction of this unit are more advanced. The 2.5-ft long vessel is made from 6 in. pipe and end caps (316 SS) welded together, and the removable water jacket has a 1/8-in annulus. An axial porous metal tube serves as the particle barrier and provides a reasonably short path for hydrogen transfer. The internal thermocouples (21) are located at three planes of elevation and are symmetrically spaced. This test bed represents a cylindrical heat transfer cell from which thermal and kinetic data will be obtained for use in the design of larger reservoirs. It will contain 84 lb of FeTi and is expected to store about 1.2 lb of hydrogen. The cost of building and operating this equipment is to be shared by the Empire State Electric Energy Research Corp. (ESEERCO), a group of nine utilities sponsoring energy research.

Progress During the Report Period: Small-Scale Test Beds: Design and fabrication of the ESEERCO test bed (B-2), the conduction-type made of 6-in. pipe, were completed; and the vessel satisfactorily passed the hydrostatic, radiographic and helium leak tests. From the several batches of commercially prepared FeTi alloy on hand, one produced by N. L. Industries was selected (NL-2) because of its lower oxygen content and relatively high storage capacity. This material was purchased as a large ingot and was physically broken up into golf ball-size chunks suitable for feed to a small mechanical crusher. The as-ground particle size distribution, excluding the 2% which was finer than 100 mesh sieve size, is given in Table 3-1. After loading the vessel with 84 lb of the alloy, the activation step was begun. This step, which slowly converts the alloy to the hydride, involves heating to nearly 600°F,

along with alternate flushing and evacuation with hydrogen, followed by cooling and contacting with hydrogen at moderate pressure (500 psia). In this step the surface becomes cleaned and microfissures develop, thus increasing the surface area for the reaction with hydrogen. Ultra-high purity hydrogen (99.999% min.) is used in the present studies, and after the first contacting 0.16 lb of hydrogen was charged. It was discharged and contacting was resumed. After 12 such cycles, essentially at room temperature, the storage capacity had increased to 0.92 lb, and contacting was continued at 500 psia. Although the activation step is time consuming, it is necessary only for the initial charge of hydrogen. If the $FeTiH_x$ should subsequently become contaminated with oxygen or moisture, its storage capacity will decrease; however, reactivation will restore its capacity. This operation proceeds much more rapidly than the initial activation and can usually be performed at a somewhat lower temperature.

During the same period work on the process lines, panel board and instrumentation was completed. All data is printed in digital form, including hydrogen pressure, flow rate and integrated flow, bed temperatures, water flow rate and inlet and outlet temperatures as well as the date and time. A view of the equipment is shown in Figure 3-1; the ESEERCO test bed is located between the panel boards. Some additional effort was necessary to eliminate small leaks which interfered with the amount of hydrogen taken up during the final stage of activation. The reaction rate was very low, and the change in supply pressure was being used to determine the amount of hydrogen uptake. From the first discharge runs it was determined that at least 1.19 lb of hydrogen had been charged during the last activation step. This amount is equivalent to the hydride $FeTiH_{1.46}$, neglecting the small amount of residual, or unavailable, hydrogen. The hydrogen was discharged during three periods of operation, the amounts being 1.046, 0.141 and 0.005 lb, respectively. The significant data are summarized in Table 3-2. In the first run the hydrogen flow rate was difficult to adjust initially because of the high differential pressure; so several minutes elapsed before a nominal flow rate of 40 LPM was established. This run was terminated when the bed pressure decreased to 33 psia. The next run was terminated when the hydrogen flow rate decreased from 40 to 34 LPM during the one-minute printing interval; and the last run was

ended when the bed pressure decreased to 19 psia. About two hours later the bed pressure had increased to 52 psia while water at 22°C was flowing through the jacket; thus some additional hydrogen could have been discharged at the 5-LPM rate. Several minor changes to aid in operation of the equipment will be made in the immediate future.

Some additional effort was put on the design of the convection-type test bed (B-1), but construction of the equipment was deferred when the long-term cyclic tests showed that the bed pressure drop increased greatly due to attrition of the $FeTiH_x$ (see Section 3.1(b)). The existing compressor which was modified for circultating hydrogen gas is now being used to reclaim cylinder hydrogen which formerly could not be utilized after the pressure decreased to 500 psia.

Task Group 3.1 (b) Metal Hydride Material Test Beds

Summary of Previous Work: Small-Scale Test Beds: Test Beds A and A-1, which were set up to study the long-term behavior of $FeTiH_x$ during hydride-dehydride cycling, had completed 840 and 266 cycles, respectively. The FeTi alloy was produced by Cannon-Muskegon Corp. (Batch No. VE 524), and charges of 386 and 380 gr, respectively, were used in the 1-in. diam. vessels (304 SS). Each cycle was conducted at a constant pressure of 530-540 psia, and hydriding proceeded for 30 min at a bed temperature of 15°-20°C (59°-68°F) followed by dehydriding for 20 min at 105°-109°C (221°-228°F). The composition change was estimated to be $FeTiH_{0.2} \rightarrow FeTiH_{1.3}$ based on the amount of released hydrogen. As expected, particle attrition increased the pressure drop; however, there was no significant decrease in storage capacity. Initially the pressure drop was about 1 in. H_2O at a hydrogen flow rate of 5000 SCCM, and when the experiment was terminated for Bed A at 840 cycles, the value was 4.7 psi. A screen analysis of the bed material showed that approximately 40% of the 20- and 30 mesh starting material (2:1 mixture) was reduced in particle size by a factor of ten. Test Bed A-1 was provided with quartz wool plugs (loosely packed) at the vessel ends in order to separate the bed from the filters.

Progress During the Report Period: Test Bed A-1 was disassembled after completing 1200 hydriding-dehydriding cycles; the extent of attrition was greater than for Bed A which went through 840 cycles. Sixty percent of the starting material was reduced in particle size by a factor of ten, and 20% had a 20-fold decrease in size. After 1080 cycles the pressure drop was 12.3 psi. The reduction in particle size did not, however, significantly decrease the ability of the bed to store hydrogen (~48 L). The high value of Δp is significant for Reference Design A, the circulating gas scheme which uses hydrogen as the heat transport medium, because it increases filtration and hydrogen circulation costs; it will have considerably less effect on the internal heat-exchange scheme (Reference Design B) because the hydrogen flow rate is very low by comparison. Examination of the test vessel at Sandia Laboratories showed that the 1200-cycle exposure caused no adverse effects. Compared with an unexposed specimen of the same 304 SS tubing, the oxide layer appeared thicker than expected. It contained Fe, Cr, O, and lesser amounts of Ni, Ti, S and C.

Two new test beds, A-1-1 and A-1-2 were put into operation for studies on the behavior of FeTi produced by N. L. Industries (Batch No. NL 1). The first bed contained 16-mesh alloy and the second one had 100-mesh alloy. They have now been through about 1400 and 1500 cycles, respectively. Their behavior has been similar to the previous pair of test beds except that their storage capacity slowly decreased over the first thousand cycles. Efforts to restore the capacity without shutting down the equipment have not been successful; so reactivation of the bed material is being considered if it is not removed for examination.

In similar equipment a series of 28 hydride-dehydride runs was made with NL-1 material in order to determine the effect of hydriding pressure and time. The initial reaction rate was very rapid due to the high driving force (difference between the charging and association pressures). For example, in a 15-min hydriding period 82% of the hydrogen reacted in 2 min at a supply pressure of 300 psia and 51% reacted at a pressure of 150 psia. The time to arrive at the composition $FeTiH_{0.4}$ was 0.61 min for a charging pressure of 300 psia, and it was 3.5 min for 150 psia. After the high initial rate

the increase in bed temperature raised the association pressure and thereby reduced the driving force; thus the reaction rate was heat-transfer limited. For the dehydriding part of the cycle, the time to reduce the composition by x = 0.4 was 13 min for material which had been hydrided for 15 min at 300 psia and was then heated to increase its pressure to 600 psia; for material which was charged at 150 psia, it took 21 min to release the same amount of hydrogen.

A new test-bed vessel made of aluminum alloy 6061-T6 was put into operation. It provides a reduced Δt between the heat-transport medium and the hydride, and it will be used for obtaining PTC equilibrium data, kinetics experiments and gas-additive effects. Furthermore, the behavior of this aluminum alloy will be determined under actual operating conditions. The temperature control will be better than that for the stainless steel jacketed vessels already in service. The vessel body was made from a piece of 4-in.-diameter barstock 1 foot long. The hydride will be contained in four 1/2-in. diameter drilled holes 90° apart, parallel to the longitudinal axis. An outer ring of twenty-four 1/4-in.-diameter holes (3-3/8 in. pitch circle) serve as channels for the heat-transport medium. Inlet and outlet headers are welded to the body ends and a flange assembly is used for the top closure. The gas line has a porous-metal filter disc (10μ rating) pressed into the head flange, and the body has an axial hole for insertion of a thermocouple from the vessel bottom to mid-height of the hydride cavities. The four cavities will hold about 200 grams of $FeTiH_x$. For the discharge of hydrogen, electrical band heaters (clamp-on type) will be used instead of steam. The association pressure vs. composition curve for $FeTiH_x$ produced from NL-1 alloy, was determined at 30°C (86°F) and is shown in Figure 3-2. Compared with the hydride made with zone-refined alloy, the plateau is narrower, and more importantly, at a 500-psi charging pressure the value of x is <0.8. Thus for the cooling water temperature of 30°C specified in Reference Design B, this material has an unusually low storage capacity.

Task Group 3.2 Safety

Scope: To investigate the safety problems of $FeTiH_x$ storage aside from the safety aspects of hydrogen gas. This activity will determine if serious safety problems exist that must be addressed in a longer range study.

Summary of Previous Work: A series of three preliminary bench-scale reservoir rupture experiments was carried out with $FeTiH_x$. No unique or unexpected safety hazards were uncovered and the material was judged to be safer than most volatile fuels. A subcontract was awarded to the Denver Research Institute to undertake a more wide ranging and definitive study of its safety characteristics.

Progress During the Report Period: A theoretical model for auto-ignition of fine metal hydride particles in air has been developed and a draft report regarding this subject was prepared. The model is successful in predicting the general trend in the variation of ignition temperature with system parameters when compared with the available experimental data for other metal systems. Unfortunately, such data are scarce and it is impossible to predict absolute values for any particular system, including $FeTiH_x$. However, the model should be helpful in the design and interpretation of experiments designed to resolve safety questions.

The Denver Research Institute study of the safety characteristics of iron titanium hydride was completed and a report issued (see Fifth Quarterly Progress Report, January 1 to March 31, 1975, BNL 20420). It was concluded on the basis of this study that the properties of this material pose no unexpected or especially serious hazard which would hinder its use as a hydrogen storage medium.

Task Group 3.3 Materials Specification and Development

Scope: Establish a set of chemical and physical specifications for iron-titanium. These specifications to include such things as partial pressure of hydrogen, particle attrition

due to hydriding and dehydriding, flow-pressure drop characteristics, sensitivity to impurities, etc., and such other properties relevant to use in hydrogen storage systems.

When preliminary specifications are available, work will begin to identify and develop the capabilities of a manufacturer to supply the quantities required for test facilities.

Summary of Previous Work: The properties of iron-titanium hydride are such that it is capable of serving as an attractive and practical energy-or-hydrogen storage medium. A pilot-scale $FeTiH_x$ reservoir, containing 879 lb of FeTi alloy and capable of storing 13 lb of hydrogen, was designed and constructed for Public Service Electric and Gas Co. of New Jersey. It replaced a tube trailer of high-pressure hydrogen at their Hydrogen-Energy Storage Test Facility and has operated successfully. Several commercial suppliers of FeTi alloy were identified and several thousand pounds were purchased.

Progress During the Report Period: The Timet subsidiary of N.L. Industries has been identified as a reliable supplier of FeTi of good quality. Two 500 lb batches of FeTi ($3/lb) were obtained from this source and our analysis of each batch is given in Table 3-3. The behavior of this material upon hydriding, as shown in Figure 3-3, approaches that of FeTi made from zone-refined, high-purity starting materials. For purposes of comparison the behavior of zone-refined material and a commercial hydride is also shown in Figure 3-3.

In the final quarter of the fiscal year, a subcontract was awarded to Internation Nickel Corp. to examine and define the interrelations among composition, microstructure and hydriding behavior of FeTi and related alloys. As part of this program some twenty alloy samples, accumulated over several years, have been examined metallurgically. These samples were characterized with respect to their hydriding behavior. All the data have not been synthesized; however, certain trends are apparent. The most important correlation is that in compounds such as $TiFe_{1-y}M_y$, where M is a transition metal, the lattice spacing expands and this expansion can be correlated with both the amount of M and the degree that the behavior of the resulting hydride departs from that of pure FeTi.

The materials development effort will be expanded in FY 1976. The rationale for this expansion is based on the following considerations. In Reference Design B the specified temperature of the available waste heat is 156°C (313°F). It has also been noted that the capital costs of a hydride energy storage unit is a sensitive function of the hydriding pressure, the cost increasing as the pressure increases. In considering these two factors one can conclude that not only is it possible to replace $FeTiH_x$ with a more stable hydride, but there is a very strong incentive to do so. The advantage, of course, lies in the fact that at any given temperature the hydriding pressure would be proportionately reduced, effecting a consequent reduction in capital costs. There are a number of ternary alloys of type $TiFe_{1-y}M_y$ which may be suitable for this purpose. However, to date we have only very limited experimental data and none of the results have been confirmed in detail; the only thing that one can say with certainty is that it is possible to produce a hydride of the type $TiFe_{1-y}M_yH_x$ which would have a substantially lower equilibrium dissociation pressure than $FeTiH_x$.

Thus the objectives of this effort are as follows:

(1) Determine the effect of the replacement of Fe on the properties of the subsequent hydride in alloys of the type $TiFe_{1-y}M_y$. Our objectives here would be to confirm previous data and to examine new alloys of potential value.

(2) Complete a detailed examination of one or more candidate systems chosen from those investigated in item (1). These systems should have properties which appear to most closely approach the optimum in relation to Reference Design B. This task should emphasize the following areas: reproducible behavior, alloy cost, kinetics, hydrogen content, hysteresis effects, and safety.

(3) Develop composition which will reduce the hysteresis phenomenon. Our objective would be to increase the understanding of the hysteresis mechanism and to apply this new insight toward minimizing hysteresis in practical energy storage systems.

Some in-house work on the metallography of FeTi has been carried out. Initial results were obtained on characterizing various batches of iron titanium alloy by means of metallography in combination with scanning electron microscopy and quantitative microprobe analysis. The chemical compositions of these materials are given in Table 3-4 and the metallographic results are briefly summarized in Table 3-5 which lists the phases present, and in some cases, their chemical composition deduced from microprobe results. The metallography work shows that the microstructure of FeTi is complex; several oxygen-bearing phases are embedded in an oxygen-free matrix of ζ FeTi. Primary dendrites having the atomic weight ratio Fe/Ti = 1.66 are common and may be ζ FeTi with a fine dispersion of ϵ Fe_2Ti. An oxygen bearing eutectic corresponding to the atomic weight ratio Fe/Ti $\sim$ 0.83 ($Fe_7Ti_{10}O_3$) occurs as a dispersed, or "Chinese-Script," phase.

For the NL alloys, the apparent result of annealing NL-1 for 16 hours at 900°C (1652°F) was to change a dendritic phase containing a few black needles to an all-black phase. The NL-2 alloy, which had the lowest oxygen content of those commercially produced, had a structure similar to the zone-refined alloy. Alloy VE-495, which had a high oxygen content, had half of the matrix covered with the "Chinese-Script" eutectic containing mixed oxide phases. Scanning electron micrographs of fractured surfaces indicated that the fracture mode is brittle and that the amounts of the oxide phases adhering to the surface correspond with the oxygen values found by chemical analysis.

It appears that the partial replacement of Fe with Mn causes little difference in the microstructure, but the hydriding behavior is modified. The Mn seems to replace the Fe in the matrix and the dendritic phase, and there is a lamellar phase having the same composition as the matrix. The alloy with 6.5% Mn did not appear to have an expanded lattice. X-ray powder patterns of the binary alloy fit the cubic structure of FeTi with a_o = 2.97 Å. The main effect of Mn on the hydriding behavior was to significantly lower the association and dissociation pressures; the characteristic pressure plateau was replaced by a sloping curve. It is of interest to note that the B-1 material which had the highest oxygen level had the poorest storage capacity; its effective capacity was only about 77% that of the zone-refined alloy.

Task Group 3.4 Selection of Container Materials

Scope: Although the 300-series stainless steels are now used successfully for the construction of small-scale hydride storage equipment, they are presently too expensive for use in large-scale plants. The reservoir environment is different from that in high pressure hydrogen systems which have been examined, due to the presence of $FeTiH_x$; consequently, suitable lower cost materials must be identified in a test program. The storage vessel must safely withstand not only the operating pressure, but it must also be resistant to hydrogen embrittlement and excessive loss of ductility.

Progress During the Report Period: Container Materials: To aid in the search for a suitable container material, a cooperative program was established with Sandia Laboratories which has carried out previous studies of hydrogen embrittlement at high pressure. Screening tests of the candidate materials in hydrogen are being performed there, and subsequently the candidate materials will be exposed in a reservoir environment at Brookhaven. The agreement also provides that Sandia supply the raw candidate materials along with drawings for the tensile specimen and its self-loading fixture. Their fabrication, and the equipment in which they are to be exposed, will be built at Brookhaven. After the specimens are tested, Sandia will examine them and make suitable recommendations. All specimens will be tested at their proofstress level in plain, notched, welded and coated forms. The first screening tests have shown that the following materials are candidates for further testing in the reservoir environment: three carbon steels A106-B, A515 Grade 70, A516 Grade 70, aluminum alloy 6061-T6, alloy steel 2¼Cr - ½Mo, and type 304 stainless steel. Further short-term tensile tests with notched bars and bars of welded material have shown that A106-B and A516 Grade 70 are the best of the ordinary steels for service on hydrogen. The use of a coating, applied to steel by a brush plating procedure, offers a way of greatly reducing hydrogen uptake in mild steel. A Pb-Sn solder coating (2 mils thick) applied to a steel specimen (10 mils thick) reduced the hydrogen permeation rate by a factor of 10^5. The effect of this coating and in air had a percent reduction in area (%RA) at

fracture of 76%. When thermally charged with hydrogen and tested in hydrogen at 600 psi, the %RA fell to 35%; but with the 2-mil coating the %RA was only 59% in hydrogen.

The hydride reservoir in which the tensile-loaded specimens will be immersed in a granular bed of $FeTiH_x$ will be called the Container Materials Test Bed, designated C-1. Construction was started on the 6-in. pipe vessel (schedule 10S, type 316 SS) which is about 2.5 ft long and accommodates 80 specimens in 8 columnar wire cages. It has an axial porous metal tube, 12 internal thermocouples, and an external water coil for handling the thermal load. The 70 lb of FeTi alloy will be activated in a companion vessel which will later be temporarily coupled to the test bed for transfer of the hydride. An accelerated operating basis consisting of about 5 hydriding-dehydriding cycles per day has been anticipated. The specimen and fixture drawings and the raw candidate materials were received from Sandia, and preparation for fabrication was started.

PROGRESS IN AREA 5: FACILITIES

Task Group 5.1 Prototype Test Facility

Scope: This Task Group contains all activities necessary to evaluate project data, and to design, construct, and operate a test facility to obtain the performance characteristics of iron-titanium beds in dynamic hydrogen systems incorporating all components necessary to prove process feasibility. All process information necessary to design and operate a Demonstration Facility is to be generated in this Task Group.

Progress During the Report Period: No further site work has been done in the proposed prototype test facility (PTF) area since the high-pressure hydrogen storage cylinders were installed. The fixed metal hydride bed with internal heat exchange surface has been selected for the PTF hydrogen storage reservoir. This process scheme is designated Reference Design B and is currently being developed in Task Group 1.2. Preliminary calculations have been made for a reservoir with a 50 kW thermal equivalent power rating and a thermal equivalent hydrogen capacity of 500 kW. These values would correspond to an estimated 20 kW(e) output from a fuel cell conversion device. On the basis of energy systems studies currently underway, the PTF may be reoriented toward dual-mode operation of the conversion device.

REFERENCES

1. F. J. Salzano, Editor, Hydrogen Storage and Production in Utility Systems, Third Quarterly Progress Report, July 1 to September 30, 1974, BNL 19520, 1974.

2. G. Kissel, P. W. T. Lu, M. H. Miles, and S. Srinivasan, Proceedings of Tenth IECEC Conference, Newark, Delaware, August 1975.

3. M. H. Miles, G. Kissel, P. W. T. Lu and S. Srinivasan, Effect of Temperature for Hydrogen and Oxygen Evolution Reactions on Nickel Electrodes in KOH Solutions, Extended Abstracts of the Toronto, Canada Meeting of the Electrochemical Society, May 1975.

4. R. D. Caton, J. Chem. Ed., 502, A571, A 574, (1974); 51, A7, A14, A16 (1974).

5. J. Giner, Electrochemical Society Journal, III, 376 (1964).

6. D. J. G. Ives and G. J. Janz (Ed.), Reference Electrodes, 103-111, Academic Press, New York 1961.

7. F. J. Salzano, Editor, Hydrogen Storage and Production in Utility Systems, Fourth Quarterly Progress Report, October 1 to December 31, 1974, BNL 20040, 1975.

8. M. H. Miles, J. Electroanal. Chem., 60, 89 (1975).

9. E. W. Brooman and A. T. Kuhn, J. Electroanal. Chem., 49, 325 (1974).

10. S. Trasatti and G. Buzzanca, J. Electroanal. Chem. 29, App. 1 (1971).

11. W. J. King and A. C. C. Tseung, Electrochim. Acta, 19, 493 (1974).

12. O. Knop, et al, Can. J. Chem., 46, 3463 (1968).

13. A. T. Kuhn and C. J. Mortimer, J. Electrochem. Soc., 120, 231 (1973).

14. S. Trasatti, J. Electroanal. Chem., 39, 163 (1972).

15. R. Parsons, Trans. Faraday Soc., 54, 1053 (1958).

16. L. I. Krishtalik in "Advances in Electrochemistry and Electrochemical Engineering," Vol. 7, P. Delahay and C. W. Tobias, Editors, Wiley, New York (1970).

17. J. O. M. Bockris and S. Srinivasan, Electrochim. Acta, 9, 31 (1964).

18. R. Haynes, Electrochim, Acta, 16, 1129 (1971).

19. D. B. Rogers, R. D. Shannon, A. W. Sleight, and J. L. Gillson, Inorg. Chem., 8, 841 (1969).

20. A. Fujishima and K. Honda, Nature 238, 37 (1972).

Table 1-1

Distribution of Costs for Reference A Design by FPC Accounts

FPC No.	Description	%
340	Land and land rights	1
341	Structure and improvements	8
342	Processing and storage equipment	72
345	Accessory electric equipment	8
346	Miscellaneous power plant equipment	1
353	Station equipment	7
	Miscellaneous construction expenses	3
		100

Table 1-2

Summary of Cost Distribution for
FPC Account No. 342

Item	%
Fuel cell packages (24) including inverters	14.3
Electrolyzer packages (24) including rectifiers	43.3
Hydride storage vessels (10)	4.6
Iron titanium hydride	15.3
Instrumentation and controls	4.5
Piping, valves, insulation, etc.	11.7
Heat exchangers, tankage and miscellaneous	6.3
	100.0

Table 1-3

The Break-Even Capital Costs of Electric Storage Devices
As a Function of the Overall Conversion Efficiency

Storage Conversion Efficiency	Distillate Oil Price $1.3/10^6 Btu			Distillate Oil Price $2.6/10^6 Btu			Distillate Oil Price $3.9/10^6 Btu		
	Load Factor	Load Factor	Load Factor	Load Factor	Load Factor	Load Factor	Load Factor	Load Factor	Load Factor
	0.05	0.10	0.20	0.05	0.10	0.20	0.05	0.10	0.20
0.05	-311	-825	-1941	-347	-896	-2048	-294	-790	1836
0.10	-16	-233	-757	-7	-216	-688	46	-110	-476
0.15	83	-36	-363	106	11	-234	159	117	-22
0.20	132	63	-166	163	125	-8	216	231	204
0.25	162	122	-47	197	193	129	250	299	341
0.30	182	162	32	220	238	219	273	344	431
0.35	196	190	88	236	270	284	289	376	496
0.40	206	211	130	248	295	333	301	401	545
0.45	214	227	163	258	314	370	311	420	582
0.50	221	240	189	265	329	401	318	435	613
0.55	226	251	211	271	341	425	324	447	637
0.60	231	260	229	276	351	446	330	457	658
0.65	235	268	244	281	360	464	334	466	675
0.70	238	274	257	285	368	478	338	474	690
0.75	241	280	268	288	374	491	341	400	703
0.80	243	285	278	291	380	503	344	486	715
0.85	245	289	287	293	385	513	346	491	725
0.90	247	293	294	295	389	522	348	495	734
0.95	249	296	301	297	393	530	350	499	742
1.00	251	300	308	299	397	537	352	503	749

All costs in 1970 dollars per kW(e). Conversion factors from 1970 dollars to 1974 and 1975 dollars are 1.313 and 1.450, respectively.

Table 2-1

Tafel Slopes, Transfer Coefficients, and Exchange Current Densities For the Hydrogen and Oxygen Evolution Reactions on Nickel Electrodes in 50% KOH at Temperatures of 80°, 150°, 208°, and 264°C.

Hydrogen Evolution Reaction

	Tafel Slope (V)		Transfer Coefficient*		Exchange Current Density (A/cm^2)	
T(°C)	low η	high η	low η	high η	low η	high η
80	0.14		0.50		1.1×10^{-4}	
150	0.054	0.28	1.6	0.30	1.8×10^{-4}	9.5×10^{-3}
208	0.070	0.32	1.4	0.30	8.0×10^{-4}	3.0×10^{-2}
264	0.066	0.20	1.6	0.53	9.3×10^{-4}	2.0×10^{-2}

Oxygen Evolution Reaction

	Tafel Slope (V)		Transfer Coefficient*		Exchange Current Density (A/cm^2)	
T(°C)	low η	high η	low η	high η	low η	high η
80	0.095		0.74		4.2×10^{-6}	
150	0.125		0.67		1.8×10^{-4}	
203	0.085	0.135	1.1	0.71	6.0×10^{-4}	3.5×10^{-3}
264	0.032		3.3		1.0×10^{-3}	

*Transfer coefficient = 2.303 RT/bF where b is the Tafel slope.

Table 2-2

Results from Testing Compounds and Alloys as Electrocatalysts for the Hydrogen and Oxygen Evolution Reactions in 30% KOH at 80°C. The Potential vs. SCE is Given Where the Current Density Attains 2mA/cm^2 Using a Sweep Rate of 50mV/sec.

Electrode	H_2(V)	Oxidation (V)	O_2(V)
TiCu	-1.25	---	0.30
Mg_2Cu	-1.30	-0.9	---
WC	-1.30	-1.1	---
TiAg	-1.40	0.0	---
VCu	-1.40	-0.9	---

Table 2-3

Tafel Parameters for the Oxygen Evolution Reaction on Nickel Based Alloys in 30% KOH at 80°C.

Material	b(volt)	α	i_o(A/cm^2)
NiAg (25 wt % Ag)	0.087	0.80	9.4×10^{-7}
NiFe (25 wt % Fe)	0.066	1.06	6.6×10^{-8}
NiCu (25 wt % Cu)	0.077	0.91	5.7×10^{-7}

Table 2-4

Kinetic Parameters for the Oxygen Evolution Reaction from 1.0 M H_2SO_4 at 80°C.

Electrode	Tafel Parameter, a (V)	Tafel Slope, b (V)	Transfer Coefficient*	Exchange Current Density (A/cm^2)
RuO_2	0.38	0.057	1.2	2×10^{-7}
Ir	0.57	0.085	0.82	2×10^{-7}
Pt	0.91	0.10	0.70	8×10^{-10}

*Transfer coefficient = 2.303 RT/bF where b is the Tafel slope.

Table 2-5

Overvoltages for Oxygen Evolution from 1.0 M H_2SO_4 at 80°C.

Electrode	ηo_2 at 20 mA/cm^2 (V)	ηo_2 at 200 mA/cm^2 (V)
RuO_2	0.29	0.35
Ir	0.41	0.50
Pt	0.74	0.84

Table 3-1

ESEERCO Test Bed Particle Size Distribution*

U.S. Std. Sieve Size	Percent of Total	Weight of Alloy Grams	Pounds
- 4 +10	66.83	25,460	56.14
-10 +16	15.18	5,784	12.75
16 +20	6.14	2,339	5.16
-20 +25	2.23	850	1.07
-25 +30	2.44	930	2.05
-30 +35	1.70	648	1.43
-35 +60	4.50	1,715	3.78
-60 +80	0.774	295	0.65
-80 +100	0.203	77	0.17
- 4 +100	100	38,100	84.0

* FeTi alloy produced by N. L. Industries, this portion designated NL2A; -4 +10 alloy is that which passed through a 4-mesh sieve and was retained on a 10-mesh sieve.

Table 3-2

Data Summary for First Discharge of ESEERCO Test Bed*

Run No.	Duration Min.	Initial/Final Conditions P psia	T °C	H_2 LPM	H_2O °C	H_2O GPM	H_2 Discharged Lb.	Total Lb.
E01D1	138	533/33	46/28	40/40	49/61	~5/~5	1.046	1.046
E01D2	19	113/19	37/19	40/34	41/39	2/2	0.141	1.187
E01D3	6	85/19	35/22	5/5	39/39	2/2	0.005	1.192

* P = pressure measured at top of bed; T = representative bed temperature based on thermocouple (No. 9) located at mid-height on the mid-area plane; H_2 flow rate is in liters/min.

Table 3-3

Analysis of FeTi Alloy Produced by N.L. Industries*

Element	NL1-B	NL2-A
Fe	57.1	55.1
Ti	43.9	43.5
O	0.32	0.051
C	0.042	0.0024

Spectrographic Results

Ni	~0.1	~0.1
Mn	~0.04	----
Al	<0.01	<0.01
Mg	<0.01	<0.001
Cr	<0.1	<0.1
Si	0.03	<0.001

*Reported as Wt. %.

Table 3-4

Chemical Composition of FeTi Materials

Material Code[1]	Wt % Fe	Ti	Mn	Al	O	C	Ni
NL1	57.1	43.9	-	-	2100	450	-
NL1 annealed	57.1	43.9	-	-	2100	450	-
NL2A-M-PC-O	55.1	45.3	-	-	410	2.4	-
B-1	52.8	44.3	-	10000	8700	1100	30000
VE-495	52.7	46.0	-	5000	2400	145	-
VE-498	38.3	54.0	6.5	1000	3000	170	-
VE-524	51.1	47.0	-	5000	3700	105	-
VE-544	49.4	47.2	2.0	30000	5100	176	-
A1014	53.8	46.2					
A1016	35.0	60.0					

[1] NL = Alloy produced by N.L. Industries.
B = Dehydrided form of a commercial hydride.
VE = Alloy produced by Cannon-Muskegon Corp.
A1014 = Zone-refined alloy (BNL).
A1016 = Fe_2Ti_4O (ENL), 5% oxygen.

THIS PAGE

WAS INTENTIONALLY

LEFT BLANK

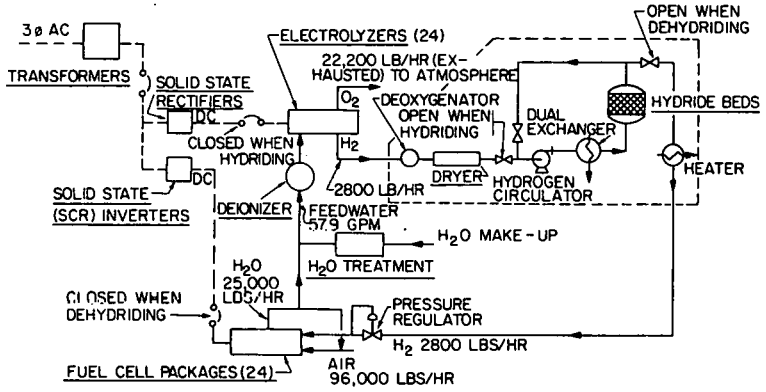

Figure 1-1. Energy storage plant process schematic.

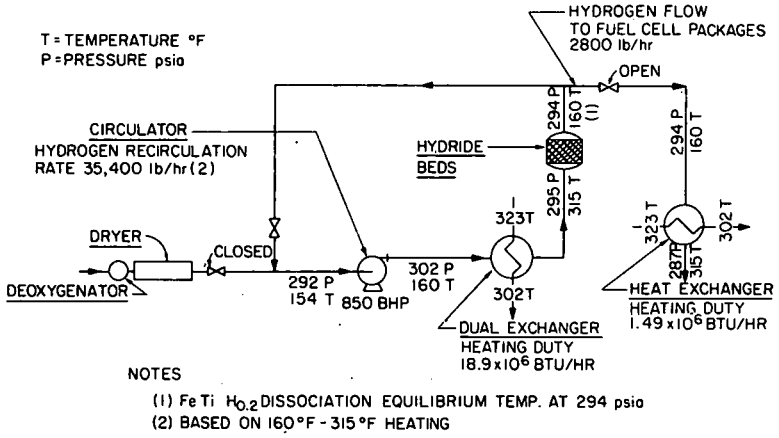

Figure 1-2. Hydriding process schematic.

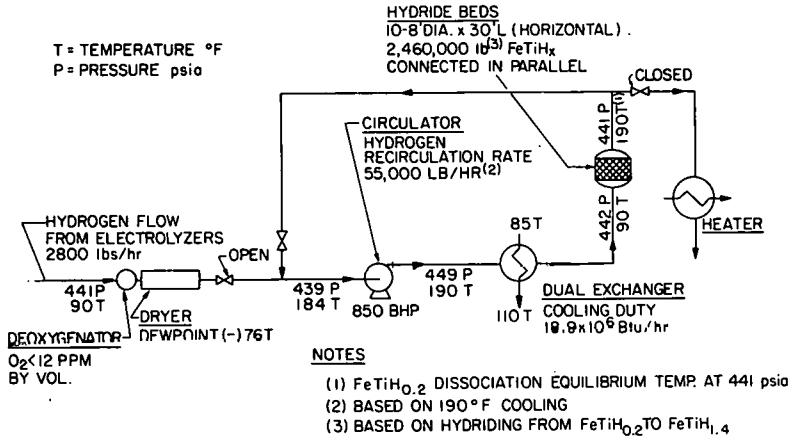

Figure 1-3. Dehydriding process schematic.

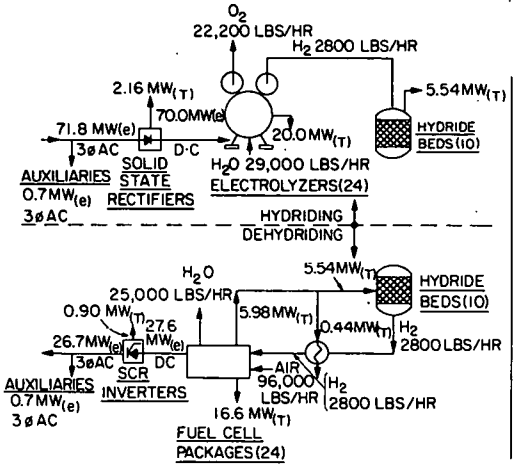

ESTIMATED NOMINAL PLANT PERFORMANCE
(CONVECTION CASE)

HYDRIDING	
RECTIFIER INPUT	71.8 MW
AUXILIARIES-(H_2 CIRCULATORS, COOLING TOWER PUMPS, OTHER PUMPS, ETC)	0.7 MW
TOTAL PLANT INPUT	72.5 MW
RATE OF H_2 ENERGY STORAGE (BASED ON HHV OF H_2)	50.1 MW
NOMINAL HYDRIDING EFFECTIVENESS	$\frac{50.1}{72.5}$ x100 = 69 %
DEHYDRIDING	
GROSS PLANT OUTPUT	26.7 MW
AUXILIARIES-(H_2 CIRCULATORS, HEATING WATER CIRCULATORS, ETC.)	0.7 MW
NET PLANT OUTPUT	26.0 MW
RATE OF H_2 ENERGY AVAILABILITY (BASED ON HHV OF H_2)	50.1 MW
NOMINAL DEHYDRIDING EFFECTIVENESS	$\frac{26.0}{50.0}$ x100 = 52 %
OVERALL PLANT EFFICIENCY	(0.69)(0.52) x100 = 36 %

Figure 1-4. Estimated plant performance based on present technology.

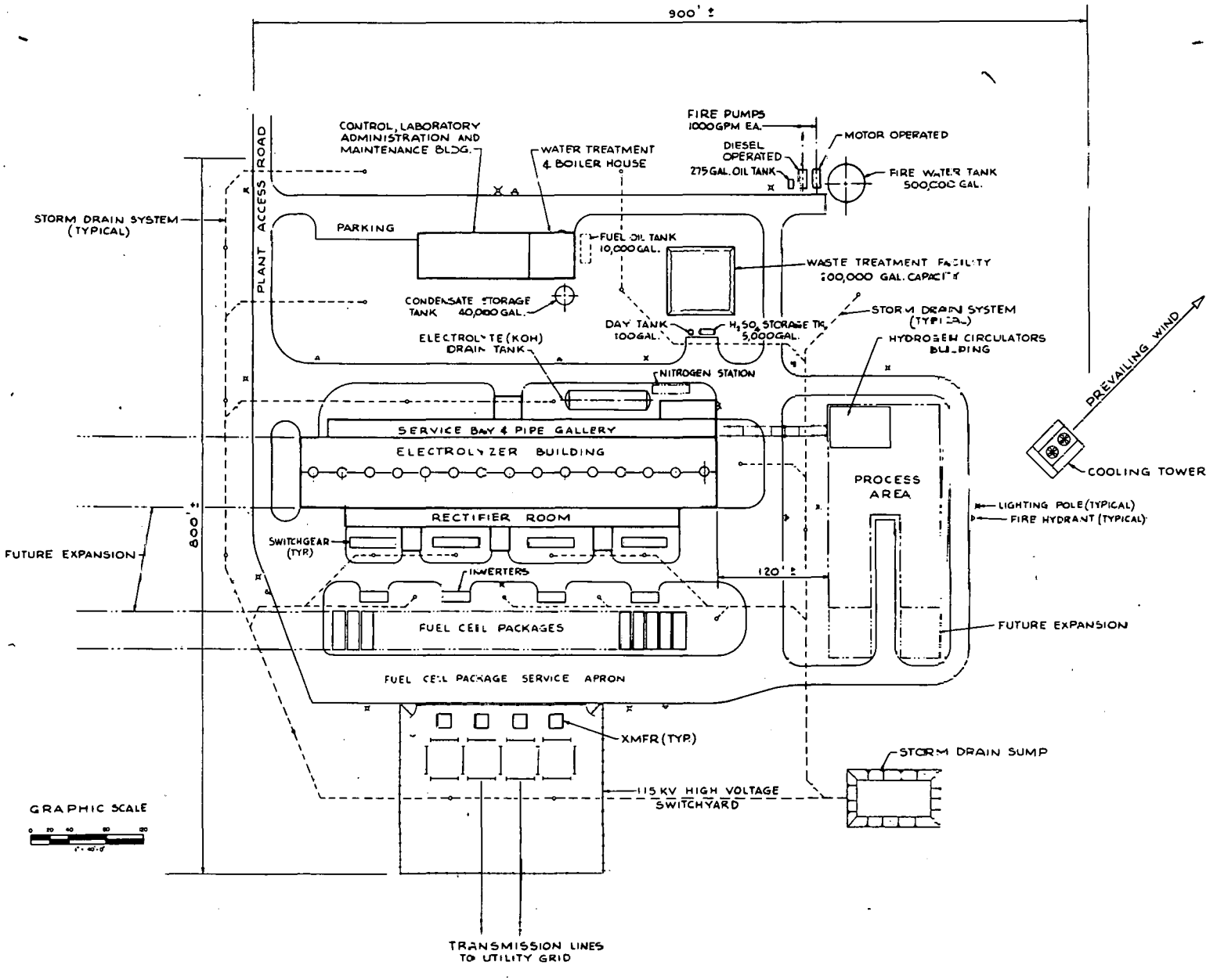

Figure 1-5. Energy storage plant site plan.

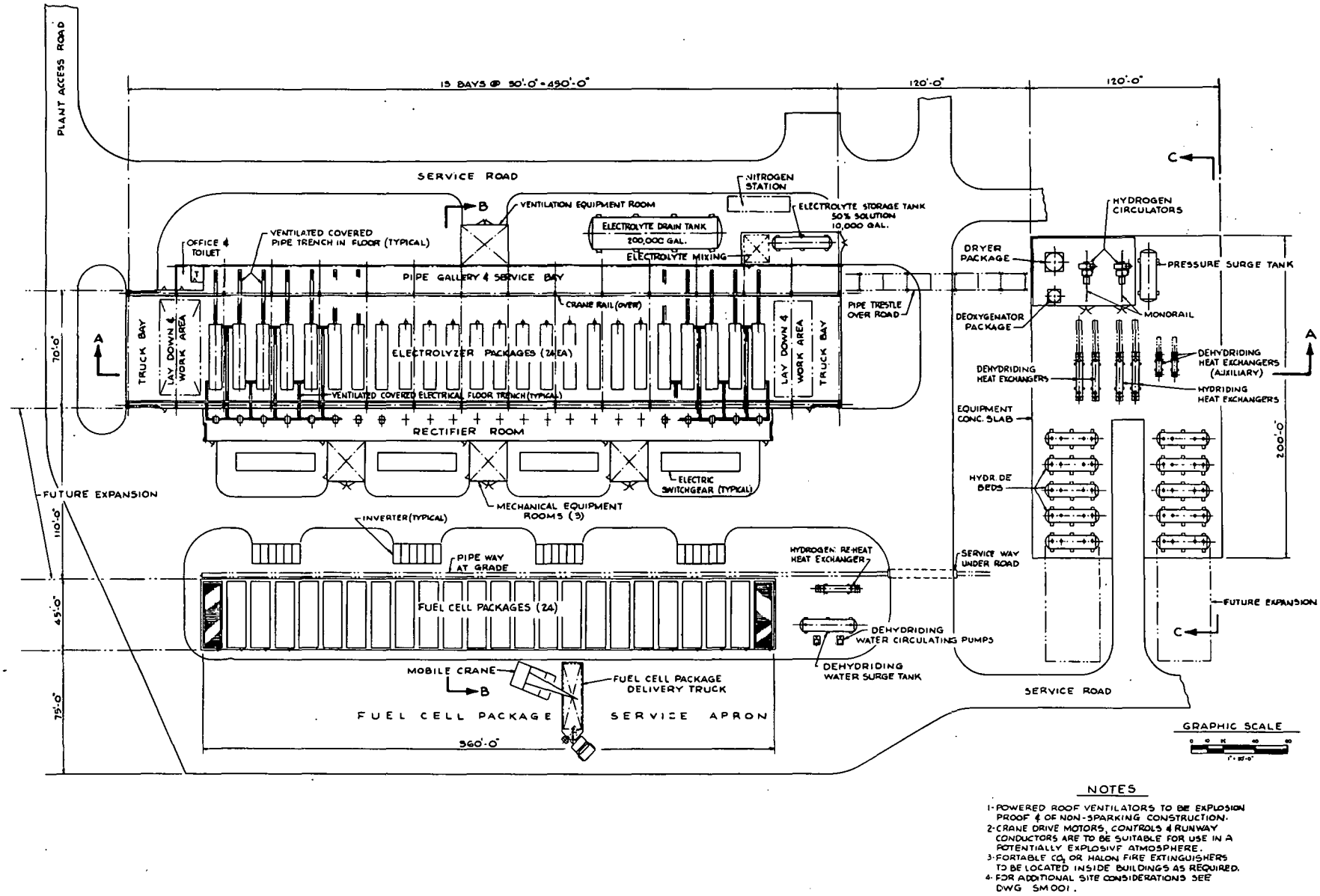

NOTES

1. POWERED ROOF VENTILATORS TO BE EXPLOSION PROOF & OF NON-SPARKING CONSTRUCTION.
2. CRANE DRIVE MOTORS, CONTROLS & RUNWAY CONDUCTORS ARE TO BE SUITABLE FOR USE IN A POTENTIALLY EXPLOSIVE ATMOSPHERE.
3. PORTABLE CO_2 OR HALON FIRE EXTINGUISHERS TO BE LOCATED INSIDE BUILDINGS AS REQUIRED.
4. FOR ADDITIONAL SITE CONSIDERATIONS SEE DWG SM001.

Figure 1-6. General plant arrangement plan.

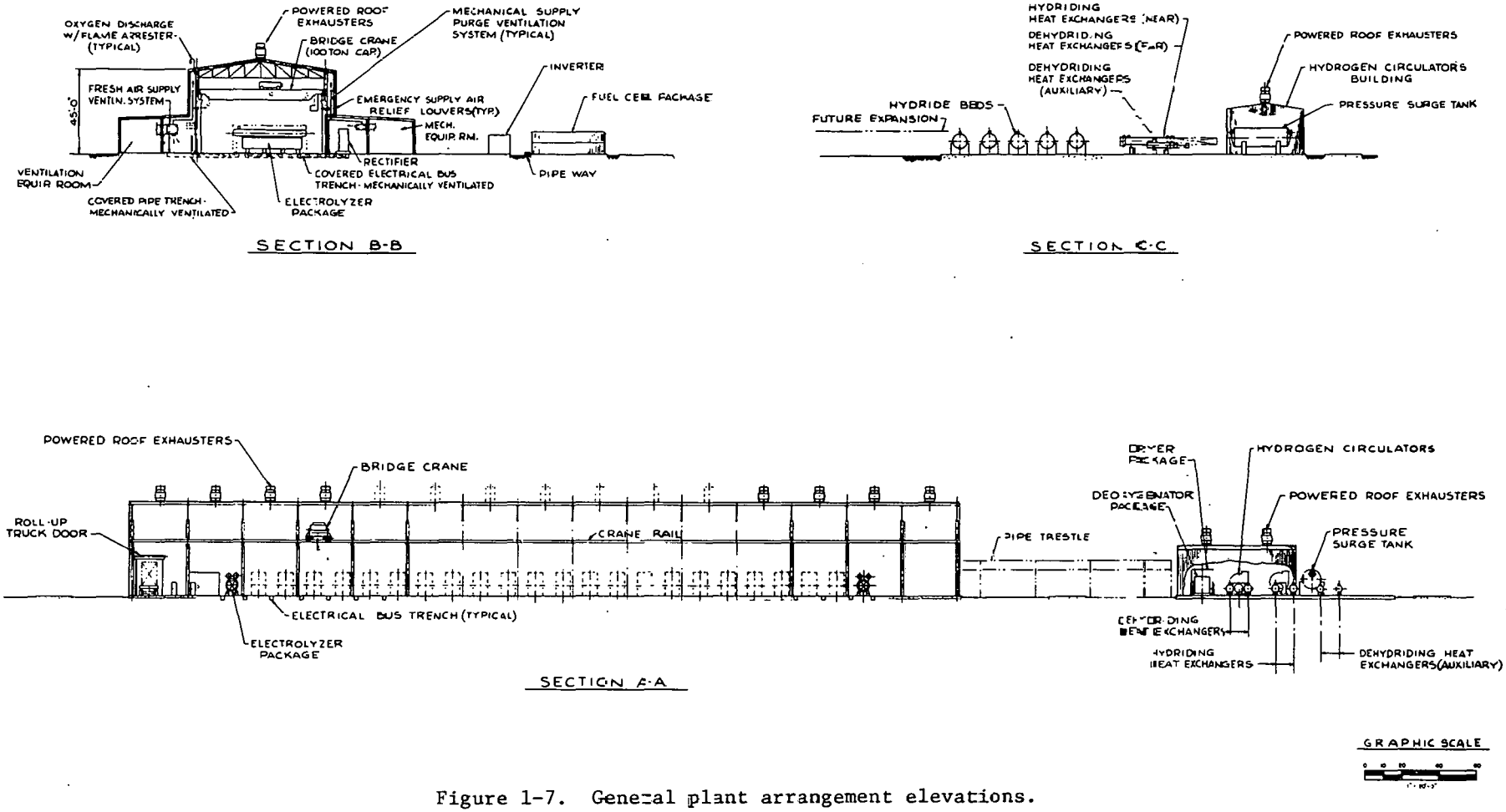

Figure 1-7. General plant arrangement elevations.

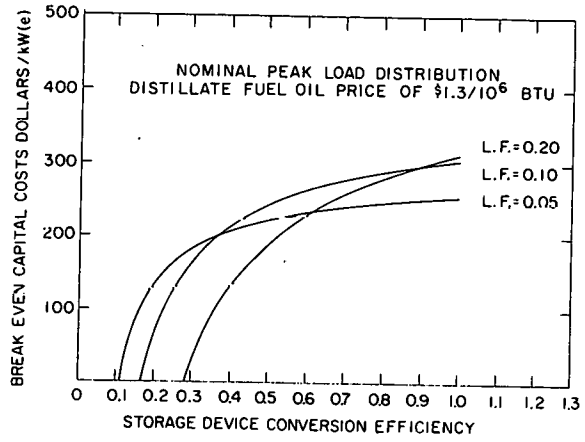

Figure 1-8. The break even capital costs of the black-box storage device, as a function of the conversion efficiency.

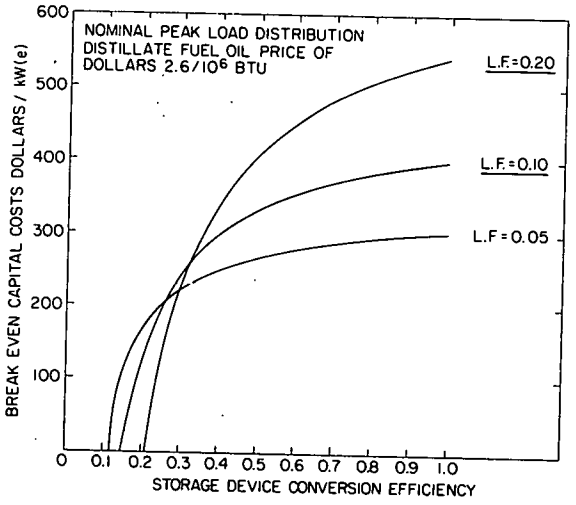

Figure 1-9. The break even capital costs of the black-box storage device, as a function of the conversion efficiency.

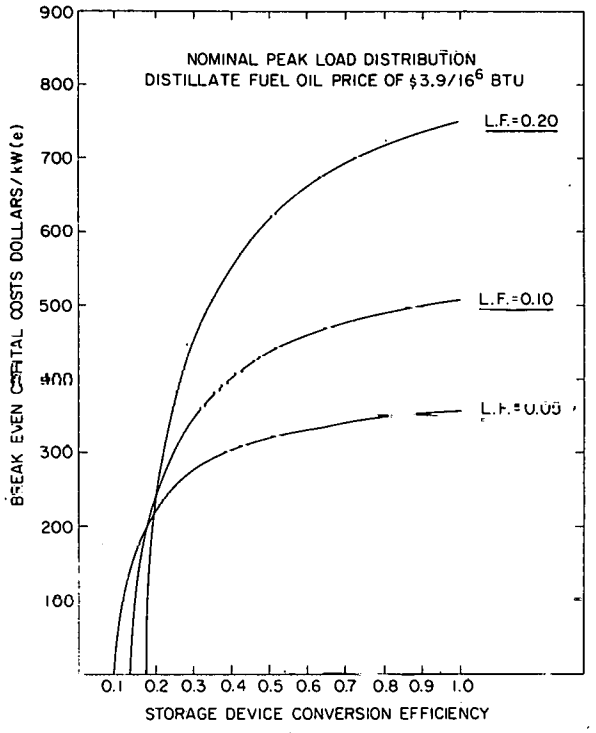

Figure 1-10. The break even capital costs of the black-box storage device, as a function of the conversion efficiency.

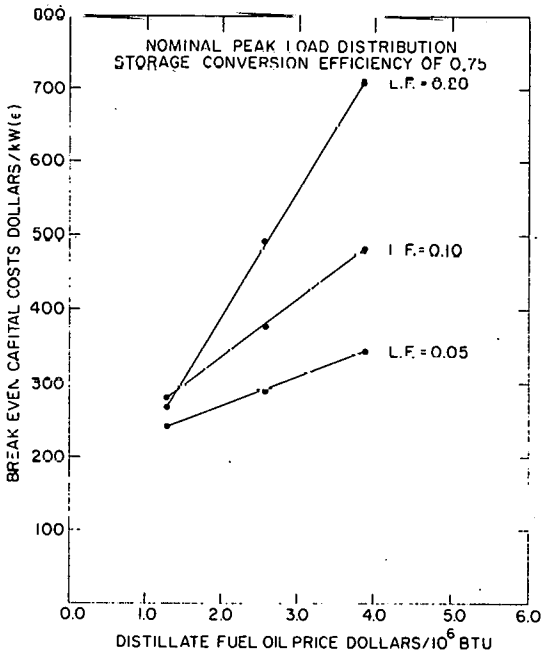

Figure 1-11. The break even capital costs of the black-box storage device, as a function of the distillate fuel oil price.

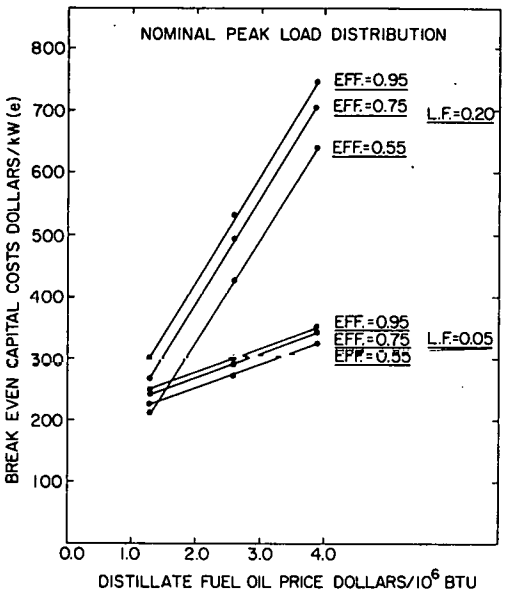

Figure 1-12. The break even capital costs of the black-box storage device, as a function of the distillate fuel oil price.

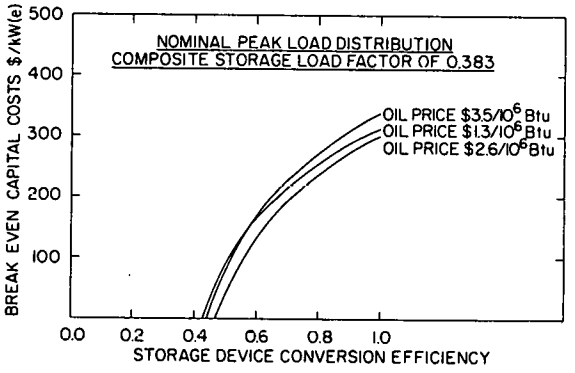

Figure 1-13. The break even capital costs of the black-box storage device, operated at both intermediate and peaking loads, as a function of the conversion efficiency.

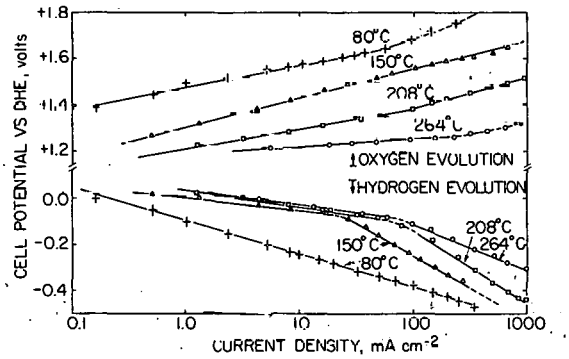

Figure 2-1. Potential vs. current density relations for hydrogen and oxygen evolution on nickel electrodes in 50% KOH solution at temperatures of 80°, 150°, 208°, and 264°C.

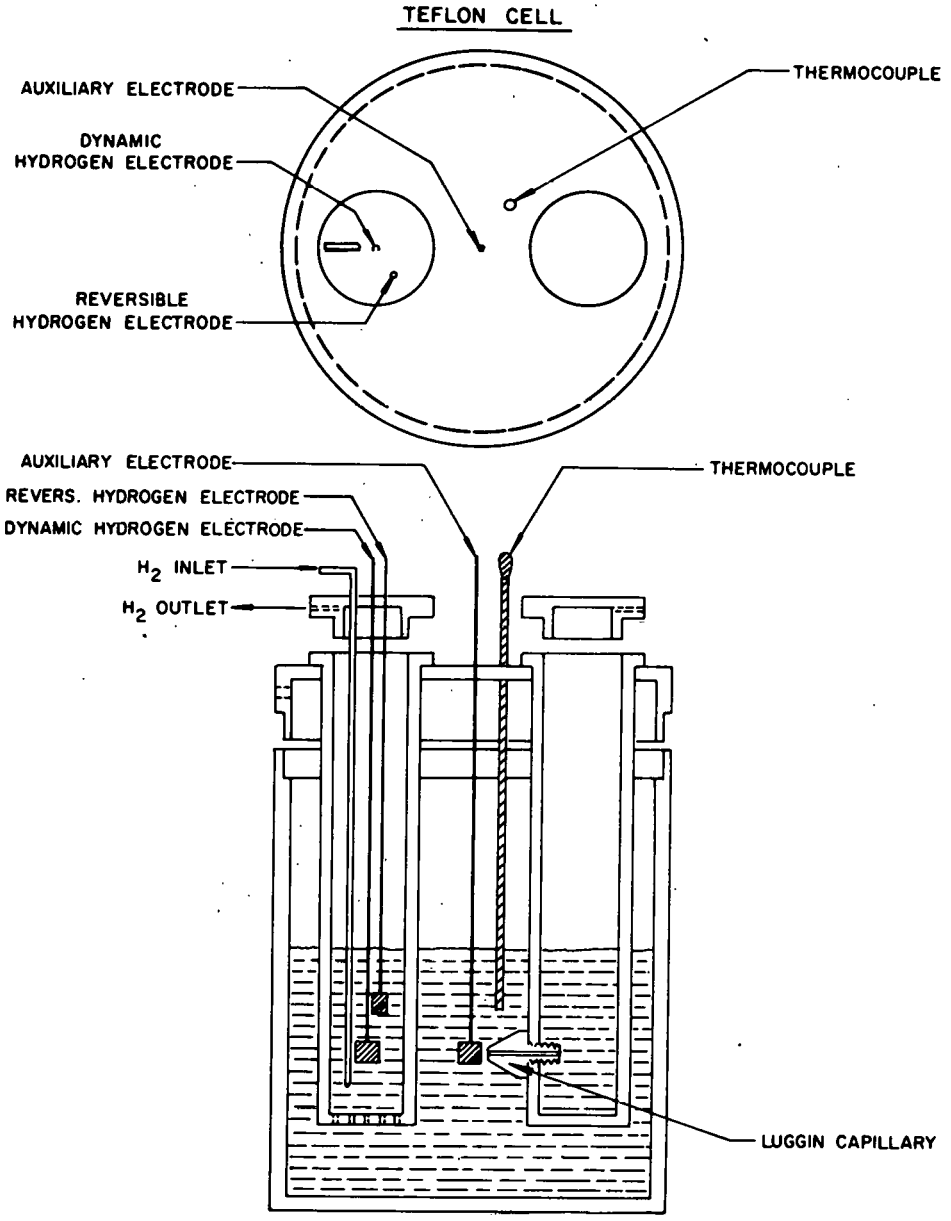

Figure 2-2. Schematic of the three compartment teflon cell.

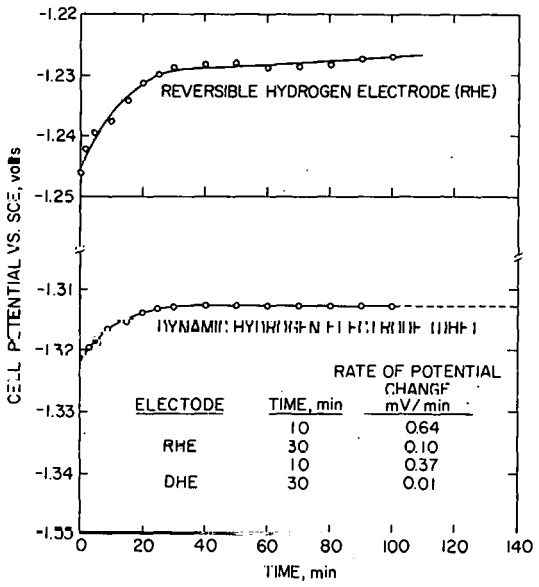

Figure 2-3. Potential of the dynamic and reversible hydrogen electrodes vs. saturated calomel electrode as a function of time in 50 wt. % KOH solutions contained in a teflon cell at 25°C.

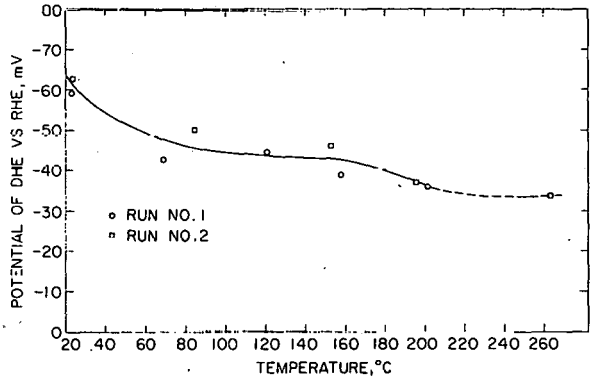

Figure 2-4. The overpotential of the dynamic hydrogen electrode in 50 wt. % KOH solution as a function of temperature.

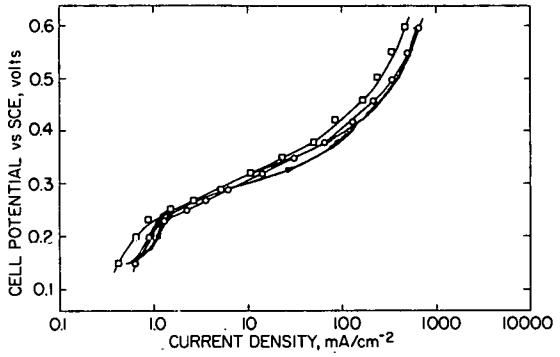

Figure 2-5. Comparison of Tafel plots from steady state potentiostatic and non-steady state voltametric measurements at sweep rate of 0.1 mV/sec for O_2 evolution reactions on Ni_3Ti in 30% KOH solutions at 80°C.

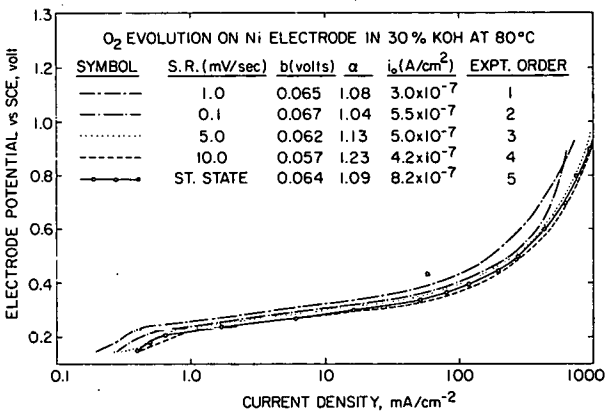

Figure 2-6. Comparison of Tafel plots from steady state potentiostatic, and transient measurements at various sweep rates for O_2 evolution reaction on Ni in 30% KOH at 80°C.

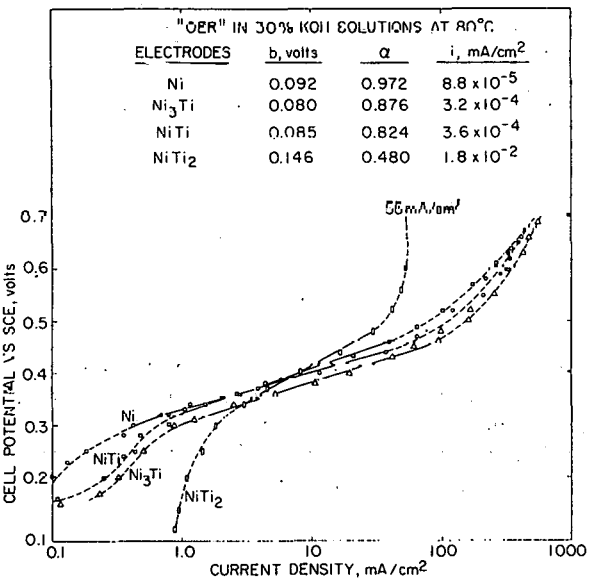

Figure 2-7. Comparison of electrocatalytic activities on Ni and NiTi intermetallic compounds for oxygen evolution from 30 wt. % KOH solutions at 80°C.

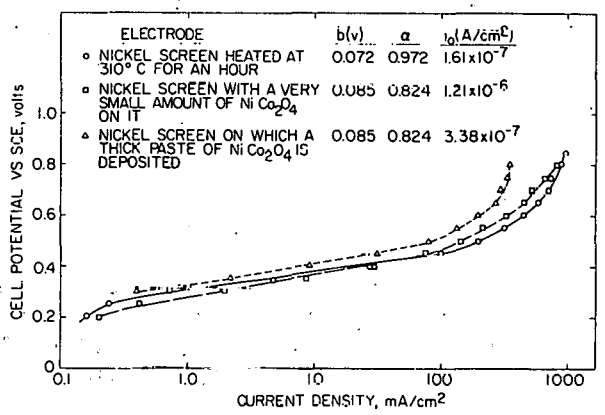

Figure 2-8. Comparison of electrocatalytic activities of Ni and teflon bonded $NiCo_2O_4$ for oxygen evolution from 30 wt. % KOH solution at 80°C.

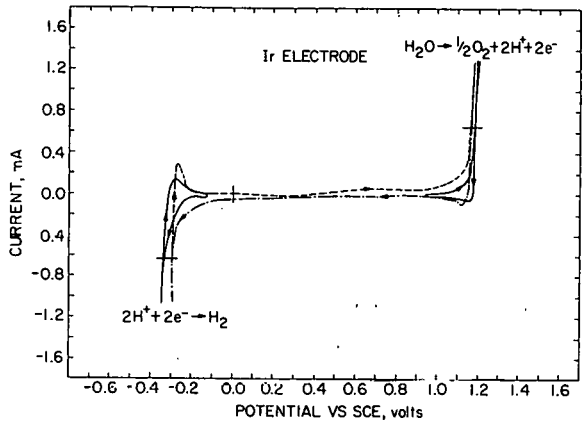

Figure 2-9. Cyclic voltammograms for an iridium electrode of 0.32 cm^2 geometrical area in 0.1 M H_2SO_4 at 80°C.

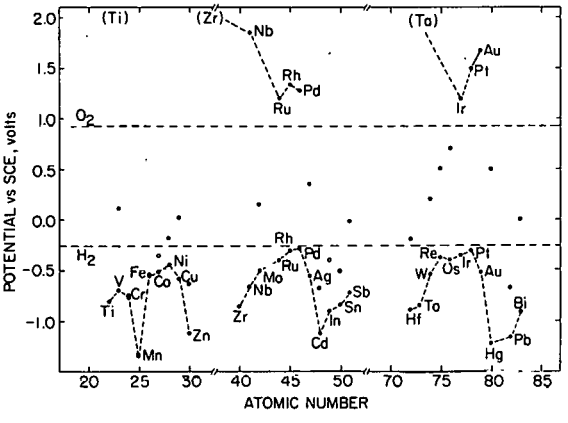

Figure 2-10. Summary of cyclic voltammetric results for various metallic elements in 0.1 M H_2SO_4 at 80°C. The potential vs. SCE is shown where the current density attains 2mA/cm^2 using a potential sweep rate of 40 mV/sec.

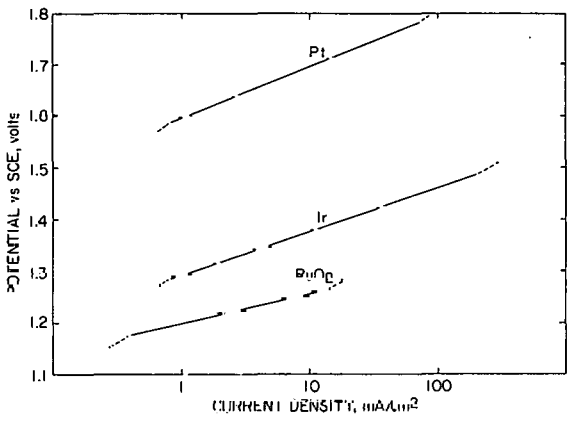

Figure 2-11. Potentiostatic steady state results for oxygen evolution on Pt, Ir, and RuO_2 in 1.0 M H_2SO_4 at 80°C.

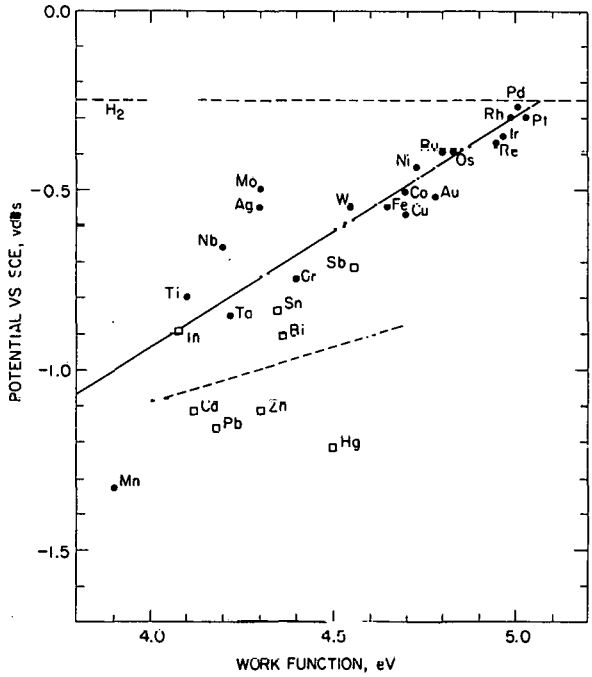

Figure 2-12. The potential vs. SCE at $2mA/cm^2$ versus the values of the work function of the metal given by Trasatti.(3) Symbols used are: • transition metals; □ sp. metals.

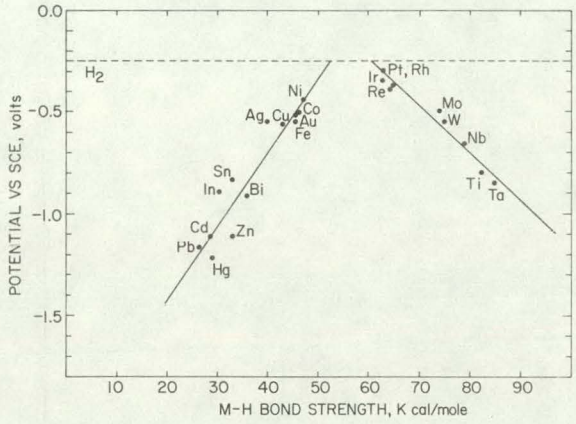

Figure 2-13. The potential vs. SCE at 2 mA/cm^2 versus the M-H bond strength as derived by Krishtalik.[5]

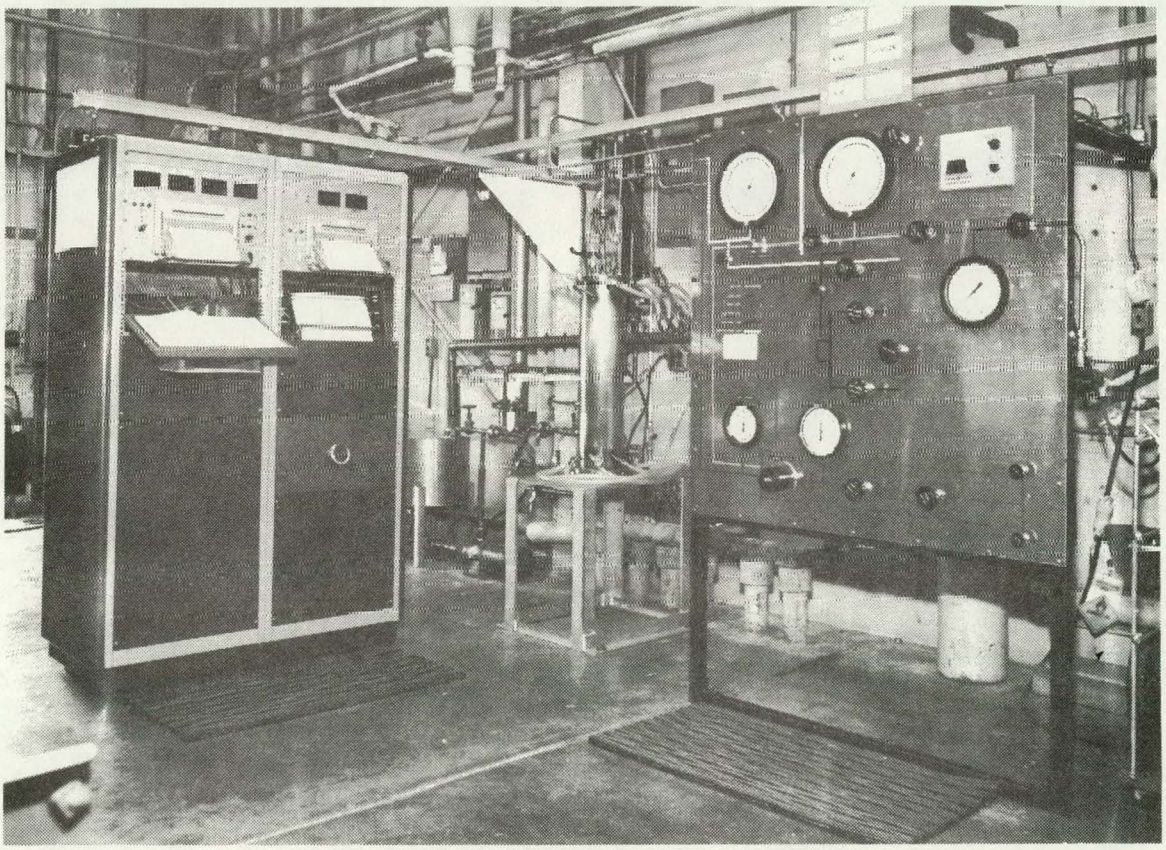

Figure 3-1. ESEERCO test bed located between panel boards.

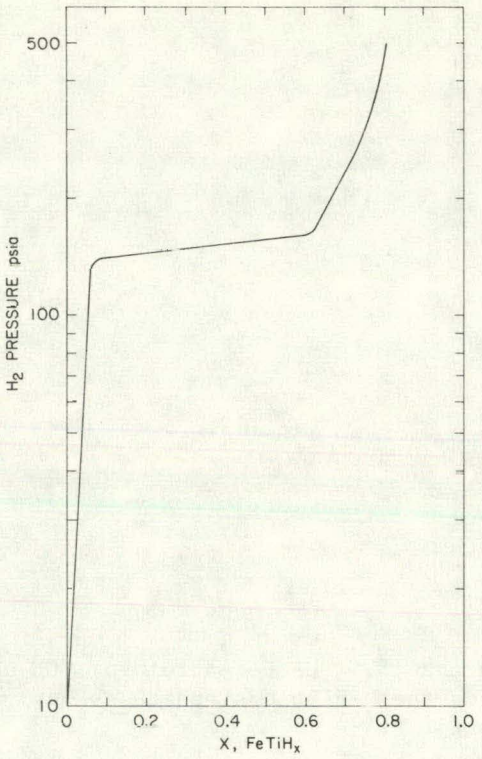

Figure 3-2. Association pressure at 30°C (86°F) vs. composition for $FeTiH_X$ produced from NL1 alloy.

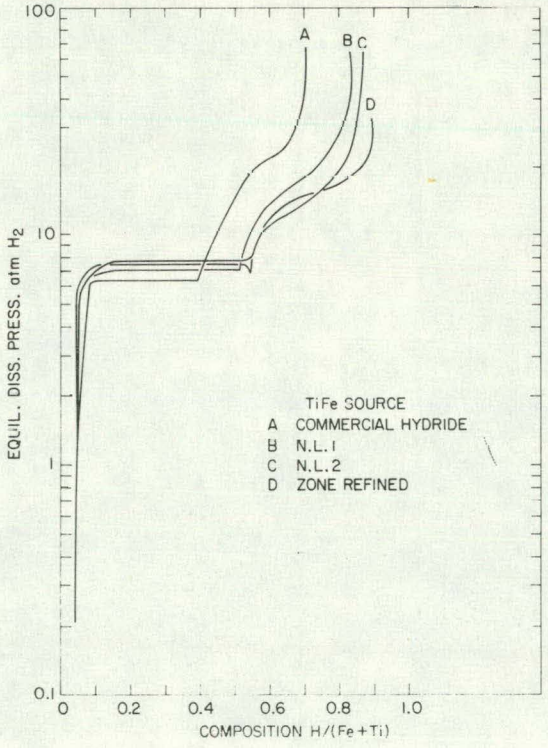

Figure 3-3. Pressure-composition isotherms at 40°C (104°F) for several iron titanium hydrides.

APPENDIX A

AREA DESCRIPTION AND LIST OF TASK AREAS

AREA 1 - Engineering Analysis and Design

This area includes the tasks that synthesize other areas of the project to generate reference designs of a Demonstration Facility (DF). The area includes the preparation of a detailed management plan for the entire program that contains manpower requirements, cost estimates, and schedules. A series of reference designs for the DF are planned. The initial design will be based on estimated performance and will serve to guide the planning of the supporting development work. As data become available from the development work, they will be factored into later reference designs. Close contact with the electric utilities will be maintained to ensure an end product that is responsive to industrial needs. Similarly, liaison with major component vendors will be established to ensure the incorporation of the latest technology into the planning and design of the facility. Analytical tools will be developed to assist in the modeling of storage systems and components. The models in turn are an integral part of system optimization studies. Also included in this area is the system analysis of energy storage as integrated into the U.S. energy economy.

Task Group 1.1 - Program Planning and Management
Task Group 1.2 - Reference Designs of Demonstration Facility (DF)
Task Group 1.3 - Liaison with Utilities and Major Component Vendors
Task Group 1.4 - Modeling of Storage System and System Optimization Studies
Task Group 1.5 - System Analysis of Energy Storage Integrated into the U.S. Energy Economy

AREA 2 - Hydrogen Production and Auxiliaries

The availability of high performance electrolytic hydrogen production units is essential to the development of electric storage via hydrogen. This area includes development work on advanced concepts such as flow-thru electrode (elimination of H_2 - O_2 separators from cells), rotating electrolysis concepts, and the evaluation, development, and scale-up of existing high performance systems. There are presently at least two advanced

electrolysis concepts now that operate well in small sizes which could be scaled to larger systems, e.g., the Teledyne Isotopes cell.

Task Group 2.1 - Test Devices
Task Group 2.2 - Vendor Development
Task Group 2.3 - Procurement of Device for Prototype Test Facility (PTF)
Task Group 2.4 - By-product Oxygen Utilization

AREA 3 - Hydrogen Storage Development

This area includes the tasks necessary to resolve problems relating to physical properties, safety, and material specifications of the chemicals required for hydrogen storage. The physical property data, particle size, pressure drop and kinetic information are important input to the modeling activity. The nature of the safety constraints must be known early in the design phase of all facilities. The preparation of purchase specifications and standards for chemicals and special materials and concurrent development of sources of supply is another early program requirement.

Task Group 3.1 - Test Beds
Task Group 3.2 - Safety
Task Group 3.3 - Materials Specification and Development
Task Group 3.4 - Selection of Container Materials

AREA 4 - Electric Generating Systems and Auxiliaries

This area covers the selection and state-of-the-art assessment of generating devices for hydrogen conversion to electric and includes fuel cells and turbines. It is essential that a high efficiency conversion device be available for inclusion in the Demonstration Facility (DF). Valuable information would be gained if a conversion device could be incorporated into the Prototype Test Facility (PTF). It is anticipated that this device will be a fuel cell and it must, of course, be representative of the state of the commercial art. However, it is possible to build and test the PTF without including a conversion device. This is an option that will be considered during the design of the PTF. There is also some industrial activity in developing hydrogen-fueled turbines of high efficiency and these must also be considered for inclusion in the PTF and DF.

Task Group 4.1 - Survey of State-of-the-Art and Specification of Alternative System
Task Group 4.2 - Vendor Development
Task Group 4.3 - Procurement of Device for PTF

AREA 5 - Facilities

This area includes the tasks necessary to design, construct, and operate the facilities required for the attainment of the project goal. The required data will come from other areas of the program. All specifications other than for the H_2 production unit, the metal hydride, and electric conversion device will originate in this Area. Two facilities are envisioned at this time: a Prototype Test Facility (PTF) and a Demonstration Facility (DF) of 25- to 50-MW(e) size. The first configuration of the PTF will validate the process conditions for an iron-titanium bed. Subsequently, hydrogen production, hydrogen conversion, and electrical gear will be added to the bed unit until the electric-to-electric PTF is completed. The operation of the completed unit will generate the final information necessary for the design, construction, and operation of the DF. The manpower and budget requirements for the DF have not been included in this Management Plan. It is anticipated that the design, construction, and operation of this facility will involve both an architect-engineer firm and Brookhaven personnel and that funding may be requested from the ERDA and appropriate utility groups such as the Electric Power Research Institute (EPRI).

Task Group 5.1 - Prototype Test Facility (PTF)
Task Group 5.2 - Demonstration Facility (DF)

APPENDIX B

PROGRAM SCHEDULE
HYDROGEN STORAGE AND PRODUCTION-UTILITY SYSTEMS

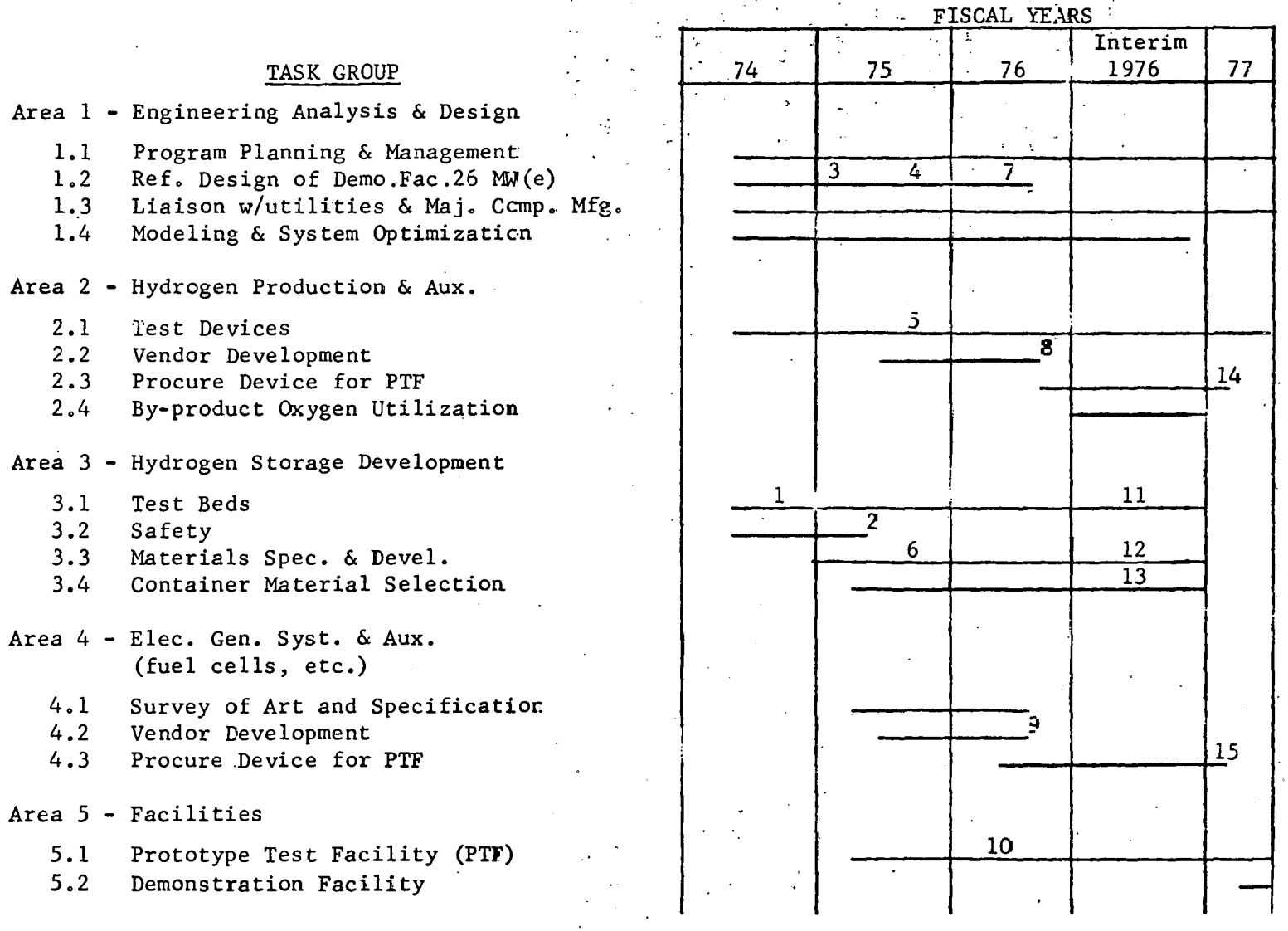

APPENDIX C

PROJECT MILESTONES

FY 1974

1. First Test Bed in operation

FY 1975

2. Extent of safety related research completed
3. Reference Design "A" completed
4. Reference Design "B" completed
5. Performance data of flow-through electrode available and concept evaluated
6. Interim specification for FeTi prototype design completed

FY 1976 and Transition Period

7. A/E plant layout and costing completed
8. Electrolysis plant for Prototype Test Facility (PTF) chosen and ordered
9. Conversion device for PTF chosen and ordered
10. Design of PTF storage vessel completed
11. Major test bed work completed
12. Specification for optimal metal hydride available and vendor chosen
13. Container material for Demonstration Facility chosen

FY 1977

14. Electrolysis plant received
15. Conversion device received

APPENDIX D

List of Existing Subcontracts

Burns & Roe	-	Engineering design and plant testing.
General Electric Company	-	For the design of a large scale water electrolysis plant based on the use of solid polymer electrolytes.
International Nickel	-	Development of specifications and large scale manufacturing techniques for FeTi alloys.
Middle Tennessee State University	-	Measurements of the catalytic properties of specific noble metal alloy systems for use in practical water electrolysis systems.
Denver Research Institute	-	Safety studies on FeTi materials.

DISTRIBUTION

ERDA Headquarters

John Belding
James Kane
Albert R. Landgrebe
Philip Lowe
James McKeown, Jr.
George Pezdirtz
F. Dee Stevenson
C. J. Swet
J. Vanderryn
Martin Zlotnick

BNL Utility Coordinating Committee

John Buechler - LILCO
Fritz Kalhammer - EPRI
Peter Lewis - PSE&G of New Jersey
Michael Lotker - Northeast Utilities